INHIBITORS OF CRD-BP-KRAS RNA INTERACTION

by

Chuyi Wang

B.Sc., Guangdong Pharmaceutical University, 2013

THESIS SUBMITTED IN PARTIAL FULFILLMENT OF
THE REQUIREMENTS FOR THE DEGREE OF
MASTER OF SCIENCE
IN
BIOCHEMISTRY

UNIVERSITY OF NORTHERN BRITISH COLUMBIA

December 2016

Abstract

The KRAS mRNA is one of few oncogenic mRNAs that can be recognized and bound by the RNA-binding protein called Coding Region Determinant-Binding Protein (CRD-BP). Binding of CRD-BP to oncogenic mRNAs can ultimately increase the possibility of tumor occurrence. Given that CRD-BP is only expressed in adult cancers but not in normal tissues, targeting the CRD-BP-mRNA interaction is a good anti-cancer strategy. To study CRD-BP-KRAS mRNA interaction and to search for inhibitors of such interaction, a safe, sensitive and high throughput-based fluorescence polarization (FP) method was developed. By using a 44 nts fluorescein-labeled KRAS RNA, a library of 217 small molecules was screened for their ability to inhibit CRD-BP-KRAS RNA interaction. Finally, candidate small molecule inhibitors as well as effective antisense oligonucleotides (AONs) against KRAS RNA were assessed for their ability to suppress KRAS gene expression in cancer cells.

Table of Contents

List of Tables

List of Figures

Acknowledgement

I would like to thank first my supervisor Dr. Chow Lee for providing me the opportunity to study this program. Dr. Chow Lee could always point me in the right direction when I feel depressed in my study, and lets me know how important persistence is in science research. I would also like to thank Dr. Maggie Li and Mr. Sebastian Mackedenski. Maggie is a trouble-shooting expert and could always provide me constructive suggestion and technical assistance. Thank Sebastian for his contribution in this research. He is so enthusiastic in science and always provide me useful tips and ideas in experiments. I would also like to acknowledge our collaborators, Ms. Chee Wei and Mr. Yeong Keng Yoon, for providing the small molecule library. Finally, I must express my very profound gratitude to my family and friends. Without their continuous support and encouragement throughout the years of my study, I would not be able to accomplish my goal. Thank you.

CHAPTER 1 Introduction

1.1 Gene expression and its relationship with diseases

In cells, genetic information is first passed from genomic DNA to RNA via transcription, and proteins are then generated through translation, as is described in the Central Dogma (Crick, 1970). Although the basic principle looks simple, gene expression is actually a very complex and delicate process. Before the genetic code within DNA is successfully expressed to functional molecules in cells, many steps including RNA editing, RNA and protein modification, RNA and protein transportation are required. However, it is difficult to ensure everything goes exactly as biologically planned in such a complex expression system. Even a slight error in any step of the gene expression process can potentially lead to disease occurrence.

It is now known that there is a close relationship between the regulation of gene expression and human diseases. Nucleotide replacement in an mRNA coding region may lead to an unpredictable change in protein sequence or structure. For instance, C to U editing in mRNA of apolipoprotein B (Apo B) induces a stop codon and changes the length of Apo B, which leads to atherosclerosis (Maas and Rich, 2000). Another example is retinitis pigmentosa, a genetic disease caused by a change in alternative splicing (Tazi *et. al.*, 2009). Non-coding RNAs (ncRNAs), such as miRNA, are also important gene regulators, as they can trigger gene silencing in RNA transcriptional, post-transcriptional regulation and chromatin modification (Taft *et. al.*, 2010). Variants in ncRNAs may also cause cancers (Hu *et. al.*, 2008; Shen *et. al.*, 2009; Calin *et. al.*, 2005) and hearing loss

(Lewis *et. al.*, 2009).

1.2 mRNA Stability and mRNA Degradation Pathways

1.2.1 mRNA decay pathways

mRNA is transcribed from genomic DNA and then used as a template in translation. When its mission is completed, mRNA is subjected to degradation. To remain stable during transcription and translation, mRNA is protected by a methylguanylate cap at its 5' end and a poly A tail at its 3' end. Eukaryotic initiation factor (eIF4E) and poly(A)-binding protein (PABP) also bind to the 5' and 3' ends respectively to help stabilize mRNA and initiate translation (Kahvejian *et. al.*, 2005, Jones *et. al.*, 1997). If mRNA is decapped, deadenylated or cleaved endonucleolytically, the body of mRNA is subjected to degradation. The mRNA decay mechanisms are critical in controlling gene expression, antiviral defenses and degrading aberrant mRNAs (Parker and Song, 2004).

There are three general mRNA decay pathways in eukaryotes, which include the deadenylation-dependent mRNA decay, the deadenylation-independent mRNA decay, and the endonuclease-mediated mRNA decay (Garneau *et. al.*, 2007). Therein, poly-A tail of mRNA would be shortened when mRNA is reused during translation procedure. Through the deadenylation-dependent mRNA decay, which is believed to be the predominant decay pathway, mRNAs are saved to some extent.

When RNA decays from 5'→3' direction in deadenylation-dependent pathway, Lsm1-7 protein complex binds to the 3'end of mRNA, which is deadenylated by CCR4 NOT complex or PARN trimer. After that, Dcp1/Dcp2 decapping protein complex decaps

the 5’ end of mRNA, resulting in a 5’→3’ decay by exoribonucleases XRN1. In 3’→5’ decay pathway, the exposed 3’end of mRNA is degraded by exosome complex. Upon decay to short oligonucleotides, mRNA is decapped by scavenger decapping protein (Garneau *et. al.*, 2007).

In deadenylatoin-independent mRNA decay, protein subunits Edc3 and Rps28B bind close to the poly A tail of mRNA, followed by recruitment of Dcp1/Dcp2 complex to decap the 5’ end (Garneau *et. al.*, 2007). Lastly, mRNA decays from the 5’ to 3’ direction by XRN1. Similar to deadenylation-dependent decay, mRNAs can be degraded from both sides in endonuclease-mediated mRNA decay pathway. But this mechanism first requires endonuclease (such as RNase MRP) to cleave within the body of mRNAs, after which mRNAs decay from both sides by the exosome complex (5’ cleaved product, 3’→5’) and ERN1 (3’ cleaved product, 5’→3’).

In addition to the general decay pathways, there are three other surveillance mRNA decay pathways that degrade aberrant mRNAs. These pathways largely help to maintain gene fidelity during translation, which further underscores the critical role of mRNA turnover in gene expression.

In the non-sense mediated decay (NMD), the exon junction complex (EJC) and the premature termination codon (PTC) are detected and trigger mRNA decay. UPF2 first binds to the EJC in the cytoplasm. When a ribosome meets PTC, it stops translation and then is bound by the SURF protein complex. UPF2 associates with SURF complex, through which EJC and PTC are joined together. Finally, SMG1 kinase phosphorylate

UPF1 located in SURF, releasing eRF1 and eRF3 and recruiting SMG7 adaptor protein, leading to mRNA decay (Garneau *et. al.*, 2007).

In the non-stop decay (NSD), when there is no stop codon and the ribosome runs through the whole mRNA until it reaches the 3' termini poly A tail. Ribosome replaces PABP, and RNA is then degraded by one of two different mechanisms according to the presence of Ski7 tRNA mimic protein. If Ski7 binds to ribosome, mRNA is released to be decayed by exosome complex from the 3' to 5' direction. If there is no Ski7, mRNA is easily decapped for the PABP absence, which results in 5'-3' decay by Xrn1 (Garneau *et. al.*, 2007).

The last surveillance pathway is no-go decay (NGD), in which Dom34-Hbs1 complex simulates endonucleolytic cleavage near the ribosome that stalled due to a strong mRNA secondary structure. The two cleaved mRNA decay products are then degraded by exosome and Xrn1 from both sides of mRNA (Garneau *et. al.*, 2007).

1.2.2 Regulators of mRNA stability: cis- elements and trans-acting factors

mRNA stability is largely controlled by two major components, the mRNA sequence itself known as cis-elements (such as iron response element, AU-rich element and sequences in the coding region) and trans-acting factors (such as ribonucleases, non-coding RNAs and RNA-binding proteins). RNA-binding proteins will be discussed in detail in section 1.3.

For example, interaction between an iron response element (IRE) and an iron regulatory protein (IRP) is necessary in regulating iron metabolism and maintaining iron

balance in an organism. When iron concentration is low in the internal environment, IRPs bind to the IREs in the 5'UTR of ferritin (an iron storage protein) mRNA, inhibiting its translation. Also, IRPs shield transferrin receptor (iron cellular uptake receptor) mRNA by associating with the IREs at its 3' UTR, preventing it from degradation (Gray *et. al.*, 1996; Binder *et. al.*, 1994).

Combination between RNA-binding protein and mRNA can largely affect mRNA stability. Over 1/3 of mRNAs contain an AU-rich element (ARE) located in their 3' UTR, which is well known as a cis-acting element responsible for mRNA turnover events. HuR protein is an RNA-binding protein that stabilizes mRNA through binding to ARE. The ARE is also a competitive binding site of mRNA destabilizing proteins, such as AUF1 and KRP. These destabilizing proteins facilitate mRNA decay by recruiting exosome complex and/or exonuclease (Garneau *et. al.*, 2007; Palanisamy *et. al.*, 2008; Chou *et. al.*, 2006). Interestingly, although AUF1 mostly promotes RNA degradation, it also has the ability to stabilize mRNAs in some cases when it functions cooperatively with other proteins (Kiledjian *et. al.*, 1997).

As mentioned in the last section, various ribonucleases, such as XRN1, PMR1 and IRE1, are involved in RNA turnover pathway. XRN1 is an exonuclease that recognizes 5'-monophosphate and cleaves decapped mRNA in all the 5' to 3' mRNA decay pathways. In endonuclease-mediated mRNA decay pathway, endonucleases including PMR1 and IRE1 cleave mRNAs which are being translated (Garneau *et. al.*, 2007).

The endogenous miRNA and the exogenous siRNA are both non-coding RNAs. In

RNA silencing, they recognize and bind to specific sequences located at mRNA coding region and lead to mRNA being sliced by RISC complexes. Targeted mRNA is complementary to siRNA or miRNA and forms a RNA duplex. It is then cleaved by Argonaute which is part of the RISC complex. The cleaved RNA is finally degraded by the same enzymes that takes part in general RNA decay pathways. Evidence also reveals that miRNA and RISC can promote mRNA decapping and repress translation initiation (Valencia-Sanchez *et. al.*, 2006).

1.3 RNA-binding proteins in the Regulation of mRNA Stability

RNA-binding proteins (RBPs) are a group of proteins that bind to multiple mRNAs either to prevent or accelerate mRNA degradation in cells. RBPs could regulate multiple RNA targets and different RBPs can bind their RNA targets specifically by recognition of RNA structure and/or sequence (Lee *et. al.*, 2006). For example, the RNA-binding protein CRD-BP can bind to various oncogenic RNAs, including c-Myc, CD44 and KRAS mRNAs (Mahapatra *et. al.*, 2013, King *et. al.*, 2014, Mongroo *et. al.*, 2011).The RNA-binding protein HuR shows high affinity to AU-rich element (ARE) of TNF-α mRNA (Chae *et. al.*, 2009). Other RBP includes the GRE binding protein CUGBP that binds to GU-rich element (GRE) to inhibit viral gene expression in cells through synergy with U1 binding protein (Goraczniak *et. al.*, 2008).

1.4 Coding Region Determinant-Binding Protein (CRD-BP)

1.4.1 Structure and Function

The Coding Region Determinant-Binding Protein (CRD-BP, also termed IMP-1/

IGF2BP1/ZBP1) is an oncofetal protein that belongs to a family of highly conserved RNA-binding protein called VICKZ (Mahapatra *et. al.*, 2013, Yisraeli, 2005). It is believed to bind to some of its target oncogenic mRNAs and to shield mRNAs from degradation. (Doyle *et. al.*, 1998).

CRD-BP has two RNA recognition motifs (RRM) and four hnRNP K-homology (KH) domains. The ~ 90 amino acids long RRM consists of two subunits call RNP-1 and RNP-2, and each of the subunits shows a β-α-β-β-α-β topology (Yisraeli, 2005). The KH domain is approximate 70 amino acids long with a β-α-α-β-β-α structure, and a conserved GXXG loop is located between α1 and α2 of the KH domain (Valverde *et. al.*, 2008). The KH domains are necessary for binding of CRD-BP. Mutations in the GXXG loop of any two KH domains of CRD-BP would result in reduced binding affinity to CRD-BP target transcripts (Barnes *et. al.,* 2015).

1.4.2 Roles in Cancer

Although CRD-BP is rarely observed in normal adult cells, it is commonly found in fetal tissues and various tumor cells, including ovarian, colon, breast, lung, testicular and brain cancers (Gu *et. al.,* 2004; Doyle *et. al,* 2000; Ross *et. al.*, 2001; Kato *et. al.*, 2007; Hammer *et. al.*, 2005; Ioannidis *et. al.*, 2004). Overexpression of CRD-BP in cells leads to increased potential of oncogenesis by promoting cell proliferation and up-regulate expression of oncogenes, suppression of cell apoptosis, as well as resistance to anticancer drugs. Evidence clearly indicates that CRD-BP is essential for oncogenesis and progression in several human cancers, through stabilization of oncogenic mRNAs which

include c-myc, ERK, GLI1, CD44 and MDR-1 (Vikesaa *et. al.*, 2006; Mahapatra *et. al.*, 2013). In an *in vitro* study, CRD-BP has been shown to prevent c-myc and MDR-1 mRNAs from endonucleolytic cleavage through shielding the coding region of mRNA (Sparanese and Lee, 2007).

1.4.3 Therapeutic Approaches against CRD-BP

Although CRD-BP is rarely observed in normal adult cells, it is over-expressed in fetal tissues and various tumor cells, including leukemia, colon, breast, pancreatic and lung cancer (Vikesaa *et. al.*, 2006; Noubissi *et. al.*, 2006; Gu *et. al.*, 2008; Ross *et. al.*, 2001; Kato *et. al.*, 2007; Hammer *et. al.*, 2005; Ioannidis *et. al.*, 2004). This suggests that CRD-BP is a very suitable target in cancer therapy (Leeds *et. al.*, 1997). Disrupting the interaction between CRD-BP and oncogenic mRNA by specific oligonucleotides (such as sense- or antisense oligonucleotides against mRNA) or small molecules would constitute a new anti-cancer strategy, and if successful, would lead to the discovery of new groups of anti-cancer compounds which act through a new molecular pathway.

Application of antisense oligonucleotide (AON) is a newly emerged anti-cancer therapeutic method. King *et.al.* (2014) designed a set of AONs against CD44 RNA to interrupt CRD-BP-CD44 mRNA interaction. Three of these AONs (DD4, DD7 and DD10) were found to specifically and effectively inhibit the binding of [^{32}P]-labeled CD44 RNA fragment to CRD-BP *in vitro*, and the cell mRNA levels of CD44 showed a roughly 60% decrease by treating cells with 100 nM of DD4 or DD7. Similarly, Mehmood *et. al.* (2016) reported an effective sense oligonucleotide (namely S1 RNA) of GLI1 mRNA showing

inhibitory effects on CRD-BP-GLI1 RNA interaction. Around 90% inhibition of CRD-BP-GLI1 RNA binding was observed by adding 147 μM of [^{32}P]-labeled S1 RNA in EMSA analysis. In addition, the mRNA levels of GLI1 and c-myc showed more than 60% decrease in 3 out of 5 cancer cell lines when cells were treated with 100 nM of S1 RNA.

Besides, the use of CRD-BP siRNAs to knock down CRD-BP RNA and protein expression was also shown to be successful in several studies. Applying 20 nM of CRD-BP siRNA was able to knockdown CRD-BP mRNA levels by 55-85% in three breast cancer cell lines and two colon cancer cell lines (Mehmood *et. al.* 2016). Mongroo *et. al.* (2011) also reported that CRD-BP siRNA inhibited CRD-BP protein expression by more than 70%. Furthermore, the CRD-BP siRNA also suppressed cell proliferation, colony size and number in colon cancer cell lines.

To date, there are only two studies reporting small molecule inhibitors of CRD-BP-RNA interaction. King *et al.* (2014) showed that while aminoglycoside neomycin was an effective inhibitor of CRD-BP-CD44 RNA interaction *in vitro*, its effect on such interaction in cells was difficult to demonstrate. This is because aminoglycosides, such as neomycin, are very positively charged and likely have affinity for many negatively charged bio-molecules such as nucleic acids in cells, leading to non-specific effects. Mahapatra *et. al.* (2013) applied a high-throughput fluorescence anisotropy screening method to identify specific small molecule inhibitors for CRD-BP-c-myc RNA interaction. They showed that 33 out of 17600 small molecules exhibited specific

inhibition on CRD-BP-c-myc RNA interaction *in vitro* and only 3 out of the 33 candidate inhibitors were effective in suppressing cell proliferation of CRD-BP positive cancer cell lines.

1.5 KRAS

1.5.1 Function and Roles in Cancer

RAS genes (HRAS, NRAS and KRAS) are a well-known family of oncogenes, which are found frequently mutated in around 1/3 of all human cancer types. They function as a transforming protein in normal tissues, delivering signals from the extracellular environment to cells. The KRAS gene encodes a 21 kDa GTPase located on the cell membrane (Friday and Adjei, 2005) and has the highest mutational rate among the three known RAS oncogenes in all human tumor diseases (Arrington *et. al.*, 2012; Bamford *et. al.*, 2004). KRAS oncogene has proven to be a critical regulator in controlling cell development, proliferation, differentiation and apoptosis, and is known to promote colon tumor cell progression (Friday and Adjei, 2005; Arrington *et. al.*, 2012).

1.5.2 Therapeutic Approaches against KRAS

Given that KRAS is highly implicated in human carcinomas, it is not surprising to see the development of therapeutic approaches targeting KRAS (Friday and Adjei, 2005). The application of AONs can result in blocked translation as well as degradation of RAS mRNA via RNase H-mediated RNA decay mechanism. Also, designed siRNAs can lead to targeted mRNA decay by catalytic activities. However, cell toxicity and the delivery of nucleic acid-based compounds such as AON an siRNA remains a major hurdle clinically

(Friday and Adjei, 2005). Therefore, researchers had started to explore other therapeutic methods, such as disrupting KRAS signaling pathway by inhibiting the expression of Raf kinase and mitogen activated protein kinase (MEK). MEK inhibitors including CI-1040, PD 0325901 and AZD6244 are in clinical trials for the possible treatment of breast cancer, colon cancer, NSCLC, or melanoma (Adjei, 2008). In addition, Dai *et. al.* (2015) noticed that tumor suppressor let-7 is able to be used as a chemosensitizer in KRAS mutated cancer cell lines. Let-7b effectively inhibited mutated KRAS expression, and decreased the IC50 of paclitaxel and gemcitabine cytotoxicity to less than half in KRAS mutant cancer cells. Inhibition of cell cycle progression, migration and invasion was also observed with the combined use of let-7 and paclitaxel/gemcitabine. Small molecules are now thought to be hopeful therapeutic agents and will be investigated as part of my research to find molecules that are capable of breaking CRD-BP-KRAS RNA interaction.

1.5.3 KRAS mRNA and its interaction with CRD-BP

CRD-BP binds directly to KRAS mRNA at its coding region and 3' UTR. KRAS was up-regulated upon overexpression of CRD-BP, while the loss of CRD-BP was shown to result in the suppression of KRAS expression and inhibition of tumor cell proliferation and anchorage-independent growth (Mongroo *et. al.*, 2011). When CRD-BP level was knocked down in cells, a protein called CYFIP2 was significantly up-regulated. Mongroo *et. al.* (2011) found that KRAS inhibition was reversed by the knockdown of CYFIP2 in the absence of CRD-BP. The study demonstrated that CRD-BP positively control KRAS expression, causing carcinogenesis potential. Also, CRD-BP level seems to be correlated

with KRAS level (Mongroo *et. al.*, 2011).

1.6 Recent Knowledge on using Oligonucleotides in Inhibiting Gene Expression

Scientists have discovered several special oligonucleotides, including AONs, siRNA and miRNA, which can be used to inhibit gene expression. In 1998, dsRNAs were found to trigger gene silencing in *Caenorhabditis elegans* and this phenomenon was termed RNA interference (RNAi) (Fire *et. al.*, 1998). siRNA and miRNA recognize and hybridize with targeted mRNA via Watson/Crick base paring, leading to mRNA degradation (Jinek and Doudna, 2009). Let-7 miRNA is a direct suppressor of CRD-BP, and can down-regulate oncogenic mRNA post-transcriptionally (Mongroo *et. al.*, 2011, Mahapatra *et. al.*, 2013). In K562 leukemia cancer cells, down-regulation of CRD-BP gene expression by specific siRNA against CRD-BP leads to increased expression of IGF-II gene (Liao *et. al.*, 2004).

With a similar fundamental principle, the AONs have been used for more than a decade to trigger RNA silencing resulting in targeted RNA decay, alternative splicing or translation inhibition (Dean and Bennett, 2003). For instance, a significant suppression of breast tumor cell progression is observed after intraperitoneal injection of AON into mice (Lamb *et. al.*, 2005). An apolipoprotein B AON was also shown to successfully reduce LDL cholesterol level in animal experiments (Crooke *et. al.*, 2005). These and many other findings showed that oligonucleotide-based therapy is indeed a promising approach for the treatment of cancers.

The use of oligonucleotides to competitively inhibit specific protein-mRNA interactions has also been explored as a new therapeutic tool in a number of diseases. In an antisense RNA intracellular study, the AONs designed to be complementary to HIV genes can bind to regulatory and structural transcript products and repress viral genome replication in an early stage (Veres *et. al.*, 1998). Examples are also found in different cancer studies. The AONs that target to a specific sequence in bcl-xL (an anti-apoptotic protein) mRNA can largely suppress bcl-xL expression in lung cancer cells (Leech *et. al.*, 2000). Two specific AONs are found to decrease bcl-xL and bcl-2 (an anti- apoptotic protein) mRNA and protein levels in malignant pleural mesothelioma, and promote cell apoptosis (Simões-Wüst *et. al.*, 2002). AONs were also shown to interrupt the interaction between c-myc mRNA and CRD-BP, downregulate c-myc expression and inhibit cell proliferation (Coulis *et. al.*, 2000). Similarly, specific AONs have been shown to inhibit CRD-BP-CD44 mRNA interaction and suppress CD44 mRNA expression in cells (King *et. al.*, 2004).

1.7 Recent Knowledge on using Small Molecules in Inhibiting Gene Expression

There is now ample evidence showing the ability of small molecules to specifically interrupt protein-RNA binding. For example, mitoxantrone can disrupt HuR-TNF-α RNA interaction. HuR RNA-binding protein stabilizes TNFα mRNA through attachment to the AREs located at the mRNA 3'UTR (D'Agostino *et. al.*, 2013). Quercetin is another potent small compound which selectively disrupt the interaction between HuR protein and ARE

in TNFα mRNA (Chae *et. al.*, 2009). In assessing HIV-1 Rev-RRE binding, small molecules including Lambda-[Ru(bpy)(2)eilatin]2+ and Delta-[Ru(bpy)(2)eilatin]2+ were shown to be efficient inhibitors of HIV-1-Rev-RRE binding as well as in HeLa plaque formation, since their structures are recognized as the RRE binding ligands (Luedtke and Tor, 2003). Small molecule antibiotics including neomycin, paramomycin, kanamycin and streptomycin were all shown to be effective in blocking CRD-BP-CD44 mRNA interaction *in vitro*. Unfortunately, such inhibition was proved to be non-specific in cells (King *et. al.*, 2014).

1.8 Goals of Research

The primary goals of my research are to find compounds, especially small organic molecules, which can inhibit the CRD-BP-KRAS mRNA interaction *in vitro*, and then assess them for their ability to inhibit KRAS expression in colon cancer cells.

To achieve my primary goals, the following four specific steps were taken: (i) I used the electrophoretic mobility shift assay (EMSA) to assess a panel of specific oligonucleotides for their ability to disrupt CRD-BP-KRAS RNA interaction, (ii) I performed a series of experiments to validate the fluorescent polarization (FP) method to study CRD-BP-RNA interaction, (iii) using the established FP method, I screened a library of small molecules for their ability to inhibit CRD-BP-KRAS RNA interaction, and (iv) I assessed candidate oligonucleotides and small molecules for their ability to inhibit KRAS and CRD-BP expression in colon cancer cell lines.

CHAPTER 2 To Identify Small Molecule Inhibitors of CRD-BP-KRAS RNA Interaction

The goal of this chapter is to identify inhibitors of CRD-BP-KRAS RNA interaction *in vitro.* The electrophoretic mobility shift assay (EMSA) was used to assess the potential inhibitory effect of 8 reverse oligonucleotides (RONs) designed against KRAS transcript on the CRD-BP-KRAS RNA interaction. RONs are direct reverse sequences of RNA where AONs are reverse and complementary sequences. By applying [^{32}P]-labeled KRAS RNA, I could determine whether CRD-BP-KRAS RNA interaction is inhibited by these RONs. This can be achieved by observing the position of the isotope-labeled free RNA and its complex.

In this Chapter, I also describe the establishment of the fluorescence polarization (FP) method to study CRD-BP-KRAS RNA interaction. I first show the proof-of-principle that the FP method can be reliably and reproducibly use to study CRD-BP-KRAS RNA interaction. The established FP assay was then used to screen a library of small molecules for their ability to inhibit CRD-BP-KRAS RNA interaction.

2.1 Methodology - Assessing reverse oligonucleotides (RONs) for their ability to inhibit CRD-BP-KRAS RNA interaction

A previous study in Dr. Lee's lab has shown that some specific sense oligonucleotides were capable of inhibiting CRD-BP-GLI1 RNA interaction (Mehmood *et. al.,* 2016). To this end, I assessed a panel of 8 specific RONs against KRAS RNA for their ability to inhibit CRD-BP-KRAS RNA interaction by applying the EMSA. The 8

RONs (see Table 2.1) were purchased from Integrated DNA Technologies, Iowa, USA.

Table 2.1 Sequences of RONs

RONs	Sequences
RON_JW1	5'-TGG TGT TCA AAT ATA AGT CAG TA-3'
RON_JW2	5'-ACG GAT GCG GTG GTC GAG GTT GA-3'
RON_JW3	5'-ATC GAC ATA GCA GTT CCG TGA GA-3'
RON_JW4	5'-AGC AGG TGT TTT ACT AAG ACT TA-3'
RON_JW5	5'-TTA GGA GAT AAC AAC CTA GTA TA-3'
RON_JW6	5'-TTA ATG ATG AAC GAA GGA CAT CC-3'
RON_JW7	5'-AGG TTC TCT GTC CAA AGA GGT AG-3'
RON_JW8	5'-AGT ACT GGA CGA CAC AGC TCT TAT-3'

2.1.1 Protein purification and quantification

Recombinant CRD-BP protein was generated in collaboration with Mr. Sebastian Mackedenski. The pET28b-CRD-BP plasmid DNA was a gift from Dr. Jeffrey Ross, University of Wisconsin. The plasmid contains a kanamycin resistance gene as well as a full length wild-type mouse CRD-BP coding sequence flanked by an amino terminus FLAG epitope and C-terminus 6 x His-tag. The recombinant protein was generated and purified using the protocol described below.

One hundred μL of E.coli BL21 (DE3) cells were stored at – 80°C and thaw on ice. One μL of plasmid DNA (~100ng) was added to the BL21 competent cells and kept on ice for 25 minutes. Cells were then heat shocked at 42°C for 90 seconds. Three hundred μL of lysogeny broth (LB) was added to the cells which was followed by incubation at 37°C for 30 minutes. Cells were then spread on a LB-Kan (25 μg/mL of kanamycin sulfate) agar plate. After the plate dried, it was covered by lid and sealed. The plate was placed in a 37°C incubator overnight in an up-side down position. The next day, about 20 colonies were picked from the plate using a pipette tip. These colonies were then swirled

in a 250 mL flask with 100 mL LB broth and 100 µL kanamycin sulfate (25 µg/mL). After cells were grown in a shaker for around 3 hours, broth was transferred to a 3 L flask and mixed with 900 mL LB broth and 900 µL kanamycin sulfate (25 µg/mL). Cells were grown on shaker again until an OD_{600} of 0.5 was reached, followed by the addition of 1 mL of 1M IPTG. After shaking for additional 6 hours, cells were spun at 3000 g at 4 °C for 15 minutes and the pellets frozen at – 80 °C overnight.

On the third day, bacterial pellets were thawed on ice for 15 minutes and resuspended in 12 mL buffer B. Cell lysate was collected in a 50 mL falcon tube and was waved (setting 4) on ice for 1 hour till solution became semi-translucent. The cell lysate was then spun at 13,200 g at 4°C for 30 minutes; meanwhile, 2 mL of nickel-nitrilotriacetic acid (Ni-NTA) agarose beads (Qiagen, Hilden, Germany) solution was added in a mini-column (Qiagen, Hilden, Germany) and was sequentially washed with 5 mL H_2O and 5 mL buffer B. The column was caped and 1.5 mL of buffer B was added to cover the resin. After centrifugation of cell lysate, supernatant was filtered (0.45 um) with a syringe into a new 50 mL falcon tube. The contents of the column were slurry and mixed with the filtered supernatant and was waved (setting 3) for another 1 hour on ice. After that, lysate-resin mixture was loaded onto the column and ready of protein purification. The mini-column was sequentially washed with 5 mL buffer B, 5 mL buffer C, and 5 mL buffer D. The column was then washed with 12 mL buffer E, and 0.5 mL of eluted solution was collected into 24 tubes. This was followed by 12 mL buffer F, and similarly 0.5 mL of eluted solution was collected into 24 tubes. All the fractions were

stored at – 80°C. Column was then washed with 6 mL 0.5 M NaOH followed by 10 mL H_2O. The washed mini-column was capped and stored in 2 mL of 30 % ethanol in the fridge.

To determine protein purification, SDS-PAGE analysis was performed on 18 fractions chosen from eluted fraction E and F. Chosen fractions were odd number tubes from fraction E3 to F13. Ten % polyacrylamide denaturing gels were prepared as according to the recipe shown in Table 2.2.

Table 2.2 Reagents used for 10% polyacrylamide denaturing gel

Lower gel mix	Volume (4 mL)
30% acylamide + 0.8%bis	1.33 mL
4x lower gel buffer	1 mL
Water	1.67 mL
TEMED	2.4 µL
20% APS	8 µL
Upper gel mix	**Volume (2.7 mL)**
30% acylamide + 0.8%bis	0.48 mL
4x upper gel buffer	0.45 mL
Water	1.77 mL
TEMED	3 µL
20% APS	7.5 µL

Sixteen µL of each protein was mixed with 4 µL of 5 x SDS sample buffer dye (containing 5% β-mercaptoethanol) prior to 10 minutes of boiling. Electrophoresis was performed at 160 volts for 55 minutes followed by gel staining with Coomasie blue on a waver for 30 minutes. Gel was then destained with destain solution (1 L destain solution consists of 50 mL methanol, 70 mL acetic acid and 880 mL H_2O) on waver for 40 minutes, and was visualized and analyzed by MultiImage® light cabinet and AlphaView software (Alpha Innotech, California, USA). CRD-BP protein fractions which have relatively good purity were selected for dialysis. Since protein was stored in 8 M urea, the refolding step

for recovering protein activity is required. One hundred μL of protein was first transferred to a 3500-molecular weight cut-off Slide-A-Lyzer® MINI dialysis unit (Thermo Scientific, Illinois, USA). The dialysis unit was then placed into 50 mL dialysis buffer A (see Table 2.3) for 24 hours in cold room. Following an overnight dialysis, the dialysis unit was placed into a 50 mL dialysis buffer B (see Table 2.3) for 4 hours followed by another 4 hour dialysis in 200 mL dialysis buffer B. Dialyzed protein was stored in 4 °C for a maximum of 2 weeks.

Table 2.3 Reagents used for Dialysis buffers

Dialysis buffer A	Volume (50 mL)
5 M NaCl	2 mL
1 M Tris-HCl (pH8)	1 mL
100% glycerol	5 mL
Urea	6 g
10% triton-X 100	50 μL
0.2 M GSH (reduced)	0.25 mL
0.1 M GSSG (oxidized)	50 μL
ddH_2O	to 50 mL
pH 7.4	
Dialysis buffer B	**Volume (250 mL)**
5 M NaCl	10 mL
1 M Tris-HCl (pH8)	5 mL
100% glycerol	25 mL
10% triton-X 100	250 μL
ddH_2O	to 250 mL
pH 7.4	

BCA assay was performed to determine protein concentration. The procedure used was according to the instructions from Pierce™ BCA protein assay kit (Thermo scientific, Illinois, USA). Briefly, albumin standard stock (2 mg/mL) was first diluted with dialysis buffer B into a set of concentrations (75 mg/mL, 125 mg/mL, 250 mg/mL, 500 mg/mL, 750 mg/mL, 1000 mg/mL and 1500 mg/mL). Working reagent was prepared by mixing 50 parts of BCA reagent A and 1 part of BCA reagent B. Twenty μL of each sample or

standard was added to 200 µL of working reagent in a 96-well plate (Sarstedt, Nümbrecht, Germany) and plate was then shaken on a plate shaker for 30 seconds prior to incubation at 37°C for 30 minutes. Following incubation, absorbance was measured at 562 nm using Synergy 2 multi-mode reader (BioTek, Vermont, USA) and analyzed with Gen5™ software (BioTek, Vermont, USA).

2.1.2 [^{32}P]-labeled KRAS RNA *in vitro* transcription

KRAS RNA was transcribed in the presence of [^{32}P]-UTP and then diluted to 25,000 cpm/µL for use in electrophoretic mobility shift assay reaction. The [^{32}P]-labeled KRAS RNA was prepared by Mr. Sebastian Mackedenski using the following protocol. The reagents shown in Table 2.4 were used for *in-vitro* transcription (IVT) reactions.

Table 2.4 Reagents used for IVT reactions

IVT reaction mixture	Volume (20 µL)
5x transcription buffer	4 µL
100 mM DTT	2 µL
40 U/µL RNasin	1 µL
10 mM ATP	1 µL
10 mM CTP	1 µL
10 mM GTP	1 µL
100 µM UTP	1 µL
DNA template	600 ng
[^{32}P]-UTP	2.5 µL
15 U/ µL T7 RNA polymerase	1 µL
DEPC water	to 20 µL

All the reagents were briefly spun down to mix and were incubated at 37°C for 1 hour. Ten µL 1 U/µL RNase-free DNase was added followed by10 minutes incubation at 37°C incubation. Ten µL urea loading dye (9 M urea, 0.01% bromophenol blue, 0.01% xylene cyanol, 0.01% phenol) was added to stop the enzymatic reaction prior to RNA gel purification. RNA mixture was run on an 8% polyacrylamide (29:1 bis:acrylamide)

denaturing gel (7 M urea) at 25 mA for 1 hour in 0.5 x TBE buffer. RNA band was sliced after gel visualization, and dissolved in 400 μL of water at 70°C for 10 minutes in a screwcap tube. RNA solution was loaded onto Performa DTR gel filtration cartridges (Edge Bio, Maryland, USA) prior to centrifugation at 3000 g for 3 minutes. The 400 μL of filtered RNA was mixed with 1400 μL 100% ethanol and 200 μL 10 X glycogen (0.2 mg/mL glycogen in 3 M sodium acetate, pH 5.2), followed by precipitation at – 20°C overnight. The mixture was then spun at 12,000 g for 20 minutes. Pellet was kept and washed with 200 μL 70% ethanol for 2 minutes, followed by ethanol removal. The dried pellet was then resuspended in 20 μL DEPC water.

2.1.3 Electrophoretic mobility shift assay competition assay

The competitive electrophoretic mobility shift assay (EMSA) was performed to assess the effectiveness of the 8 KRAS RONs to compete with the [^{32}P]-labeled KRAS RNA in binding to CRD-BP. The RONs were assessed with 10 X and 50 X molar excess of the [^{32}P]-labeled KRAS RNA. The same molar excess of the unlabeled KRAS RNA were used as positive controls. Reagents for EMSA reaction are shown in Table 2.5.

Table 2.5 Reagents for EMSA reaction

EMSA binding buffer	Volume (1 mL)	
1 M Tris-Cl (pH 7.4)	50 µL	
0.5 M EDTA (pH 8.0)	25 µL	
100 mM DTT	100 µL	
50% Glycerol	500 µL	
10% Triton-X 100	1 µL	
ddH_2O	324 µL	
EMSA reaction reagent	**Volume (17 µL)**	**Final concentration**
EMSA binding buffer	4 µL	
Baker's yeast tRNA (25 mg/ mL)	1 µL	
BSA (10 mg/ mL)	1 µL	
RNasin (40 U/ µL)	1 µL	
CRD-BP	7 µL	217 nM
[^{32}P]-labeled KRAS RNA	2 µL	118 pM
Competitors	1 µL	1.18 nM and 5.9 nM

EMSA binding buffer was divided into aliquots and stored at –20 °C. The [^{32}P]-labeled KRAS RNA was refolded by heating to 55 °C for 5 minutes followed by cooling to room temperature for 7 minutes. All the reagents for EMSA reaction were added on the side of microcentrifuge tube and spun down in 1.5 mL centrifuge tubes to start reactions. The mixture was then incubated at 35°C for 10 minutes followed by incubation on ice for 5 minutes. Such warm-cool incubation step was repeated one more time to complete the binding reaction. Two µL of EMSA loading dye was added to each centrifuge tube prior to loading onto an 8% polyacrylamide gel (29:1 bis:acrylamide) non-denaturing gel in 0.5 x TBE running buffer. The gel was subjected to electrophoresis for 55 minutes at 25 mA. EMSA gels were typically exposed onto phosphor screens overnight at -80°C and images visualized using a Cyclone Storage Phosphor Imager system (Packard Instrument Company, Connecticut, USA) using Optiquant software version 4.0 (Packard Instrument Company, Connecticut, USA).

2.2 Methodology - Screening small molecule inhibitors for ability to inhibit CRD-BP-KRAS RNA interaction

The fluorescence polarization (FP) method must first be established, in order to conveniently study the CRD-BP-KRAS RNA interaction and to screen a library of small molecule for their ability to inhibit CRD-BP-KRAS RNA interaction. The library of small molecules consisted of 217 dispiro pyrrolizidine/indanone derivatives were then assessed by the FP method to identify potential inhibitors of CRD-BP-KRAS RNA interaction.

2.2.1 Establishing the Fluorescence Polarization method to study CRD-BP-KRAS RNA interaction

At the outset of this study, Dr. Lee's lab has mapped the smallest region of both CD44 (King *et. al.,* 2014) and KRAS (Sebastian Mackedenski, unpublished results) RNAs that are still capable of binding to CRD-BP. Based on these previous studies, a 39-nt fluorescent-labeled CD44 (FL-CD44) RNA (5'- AAA UUA GGG CCC AAU UAA UAA UCA GCA AGA AUU UGA UCG /Fl/ -3') (Thermo Scientific, Illinois, USA) and a 44-nt fluorescent-labeled KRAS (FL-KRAS) RNA (5'- AUG GAG AAA CCU GUC UCU UGG AUA UUC UCG ACA CAG CAG GUC AU/ 36FAM/ -3') (Integrated DNA Technologies, Iowa, USA) were commercially synthesized. In addition, Dr. Lee's Lab has designed eight antisense oligonucleotides (AONs) against KRAS mRNA and found two AONs that could block CRD-BP-KRAS mRNA binding *in vitro* (Sebastian Mackedenski, unpublished data). One of the two inhibitors, SM7 (5'-UCC AAG AGA CAG GUU UCU CCA UC-3') (Integrated DNA Technologies, Iowa, USA), was used as a positive control

in my experiments described in this thesis. SM2 (5'-UGC CUA CGC CAC CAG CUC CAA CU-3') (Integrated DNA Technologies, Iowa, USA) which had no effect on CRD-BP-KRAS RNA interaction, was chosen as a negative control in the FP assay. And the concentration of both AONs used in the FP assay is 500 nM.

Wild-type (WT) CRD-BP was purified and quantified using the protocols described in section 2.1.1 and its corresponding recombinant KH variants were provided by other member in the Lee Lab. The CRD-BP variants, KH1-2, KH3 and KH3-4, harbor single or double point mutations in the first glycine of the *GXXG* conserved motif located in each KH domain of CRD-BP (Barnes *et. al.,* 2015). Structures of CRD-BP and KH variants are shown in Figure 2.1.

Figure 2.1 Schematic diagram of CRD-BP. CRD-BP consists of 2 RNA recognition motifs (RRMs) and 4 K homology (KH) domains. Point mutation occurs in *GXXG* motif on KH domains. KH1-2 harbors a point mutation on KH1 and KH2 domains respectively. KH3 harbors a point mutation on KH3 domain. KH3-4 harbors a point mutation on KH3 and KH4 domains respectively.

Several concentrations of fluorescent-labeled RNAs were tested on a fixed concentration of CRD-BP in the FP assay to determine the optimal assay concentration. The KH variants of CRD-BP have been shown to have deficiency in binding to KRAS (Sebastian Mackedenski, unpublished observations) and/or CD44 RNAs (Barnes *et. al.,*

2015) as determined using the [^{32}P]-labeled EMSA. To assess the specificity of CRD-BP-RNA binding and to determine the suitable working concentration for small molecule screening, the binding profile of CRD-BP wild-type and its KH variants were studied using the FP assay.

CRD-BP WT and KH variants were diluted to designated concentrations with dialysis buffer B. The concentrations of CRD-BP WT and KH variants used in experiments were described here.

Table 2.6 Reagents used for FP assay

FP binding buffer	Volume (1 mL)	
1 M Tris-Cl (pH7.4)	50 µL	
0.5 M EDTA (pH8.0)	25 µL	
50 % Glycerol	500 µL	
10 % Triton-X 100	1 µL	
ddH_2O	424 µL	
FP assay reagent	Volume (19 µL)	Final concentration
FP binding buffer	4 µL	
CRD-BP	7 µL	0-1000 nM
fluorescent-labeled RNA	5 µL	10 nM
ddH_2O	3 µL	

All the reagents (see Table 2.6) for FP assay were pipetted into a 384 Microfluor 1 Microtiter® plate (Thermo Electron, Massachusetts, USA) and incubated at 37°C for 10 minutes followed by 5 minute on ice bath. Reaction tubes were then incubated again at 37°C for 10 minutes and 5 minutes on ice bath prior to plate reading. Plate was read (485/20 excitation light, 528/20 emission light) using Synergy 2 multi-mode reader (BioTek, Vermont, USA) and analyzed with Gen5™ software (BioTek, Vermont, USA).

2.2.2 Screening a small molecule library for ability to inhibit CRD-BP-KRAS RNA interaction

After the establishment of the FP method, I proceeded to screen the library of small

molecules for their ability to disrupt CRD-BP-KRAS RNA interaction, namely by measuring any decrease in FP units as an indicator of disruption of CRD-BP-RNA interaction. The library of small molecules that I assessed consists of 217 dispiro pyrrolizidine/indanone derivatives. These were obtained from the University Sains Malaysia. Dr. Lee's lab has previously identified two antisense oligonucleotides, SM7 and SM6, which are effective inhibitors of CRD-BP-KRAS RNA interaction (Sebastian Mackedenski, unpublished results), while SM2 antisense oligonucleotide had no effect. Therefore, I used these antisense oligonucleotides as controls in my screening experiments. Since the small molecules were resuspended in DMSO, I also assessed various concentrations of DMSO on FP measurements to determine the concentration at which DMSO has effect on FP measurements. Each small molecule was assessed with a fixed concentration during the primary screening process.

Table 2.7 Reagents used for small molecule library screening

FP assay reagent	Volume (19 µL)	Final concentration
FP binding buffer	4 µL	
CRD-BP	7 µL	500 nM
fluorescent-labeled RNA	2 µL	10 nM
small molecule	4 µL	100 µM
ddH_2O	2 µL	

The contents in FP binding buffer are shown in Table 2.6. All reagents (Table 2.7) for library screening were first mixed together to make a master mix, except for the small molecules. Small molecules were then pipetted into a 384 Microfluor 1 Microtiter® plate (Thermo Electron, Massachusetts, USA) followed by addition of the master mix. Incubation steps for CRD-BP-KRAS RNA binding reaction followed the same procedure as those described in section 2.2.1.

Dose-dependent assays of small molecule inhibitors were performed after candidate inhibitors were identified from the primary screening step. Selected small molecules were diluted from 0 to 100 μM with DMSO and incubated with fixed concentration of KRAS RNA and CRD-BP WT.

2.3 Results and Discussion

2.3.1 EMSA Competition assay

The eight RONs (Table 2.1), designed by Dr. Lee, are reverse oligonucleotides against the KRAS transcript nts 1-186. It was previously shown that sense oligonucleotides against GLI1 mRNA could inhibit interaction between CRD-BP and the truncated GLI1 mRNA (Mehmood *et. al.,* 2016). Both sense oligonucleotide and RON were postulated to imitate KRAS mRNA secondary structures and be recognized by CRD-BP, thereby competing with KRAS transcript in binding to CRD-BP. Therefore, it would be of interest to assess if RONs against KRAS mRNA can inhibit CRD-BP-KRAS RNA interaction. Because RON is a direct reverse sequence of an RNA, the nucleotides that account for hairpin structures are still the same. The KRAS RNA substrate used in the EMSA was a truncated binding region corresponding to nts 93-185 that still has affinity for CRD-BP (Sebastian Mackedenski, unpublished data). The unlabeled KRAS RNA used as a positive control competitor RNA has the same sequence as the [^{32}P]-labeled KRAS RNA nts 93-185.

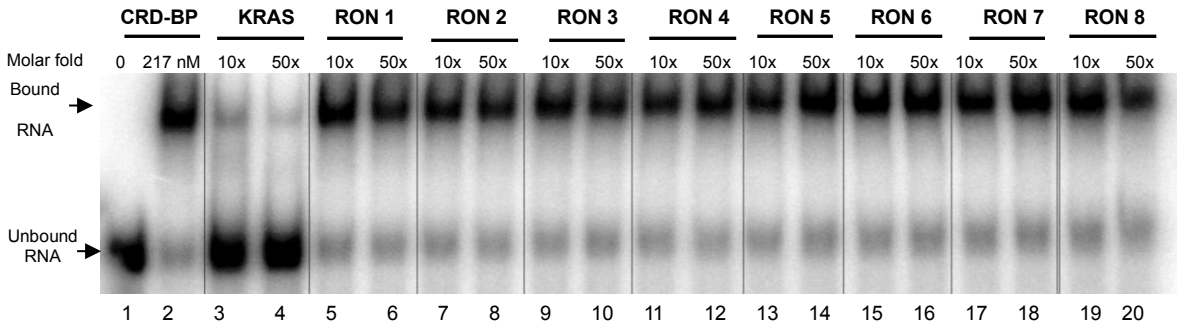

Figure 2.2 Assessing KRAS RONs for ability to compete with the [32P]-labeled KRAS RNA nts 93-185 for binding to CRD-BP. 118 pM of [^{32}P]-labeled KRAS RNA (lane1) was mostly gel shifted by 217 nM of CRD-BP (lane 2). Unlabeled KRAS mRNA was 10 molar-fold (1.18 nM) and 50 molar-fold (5.9 nM) of [^{32}P]-labeled KRAS RNA (lanes 3 and 4). RON competitors (lanes 5-20) were assessed with 10 molar-fold (1.18 nM) and 50 molar-fold (5.9 nM) excess of the [^{32}P]-labeled KRAS RNA. The results shown is a representative of three separate experiments (n=3).

As shown in Figure 2.2, at 10- and 50-fold molar excess none of the RONs showed any ability to block the binding of CRD-BP to [^{32}P]-labeled KRAS RNA (lanes 5-20). This suggests that RONs of KRAS did not compete with [^{32}P]-labeled KRAS RNA for binding to CRD-BP. The length of each RON is 23 nts (except RON_JW8 is 24 nts) and it is possible that larger sized RONs against KRAS mRNA are required to obtain sufficient thermodynamic free energy to form and mimic the secondary structure of KRAS mRNA. Alternatively, the differences between the KRAS and CD44 RONs could be due to the differences in the binding of these transcripts to CRD-BP (Sebastian Mackedenski, unpublished observation).

2.3.2 Binding profiles of WT CRD-BP and variants

A previous study on CRD-BP KH variants showed that any double point mutations on CRD-BP, except KH3-4, lost their binding affinity for CD44 RNA, while single point-mutated CRD-BP maintained the RNA binding ability (Barnes *et. al.,* 2015). To

validate the FP assay for studying CRD-BP-RNA interaction, the KRAS and CD44 RNA binding curves of CRD-BP variants and WT-CRD-BP were compared. The FP results are shown in Figure 2.3.

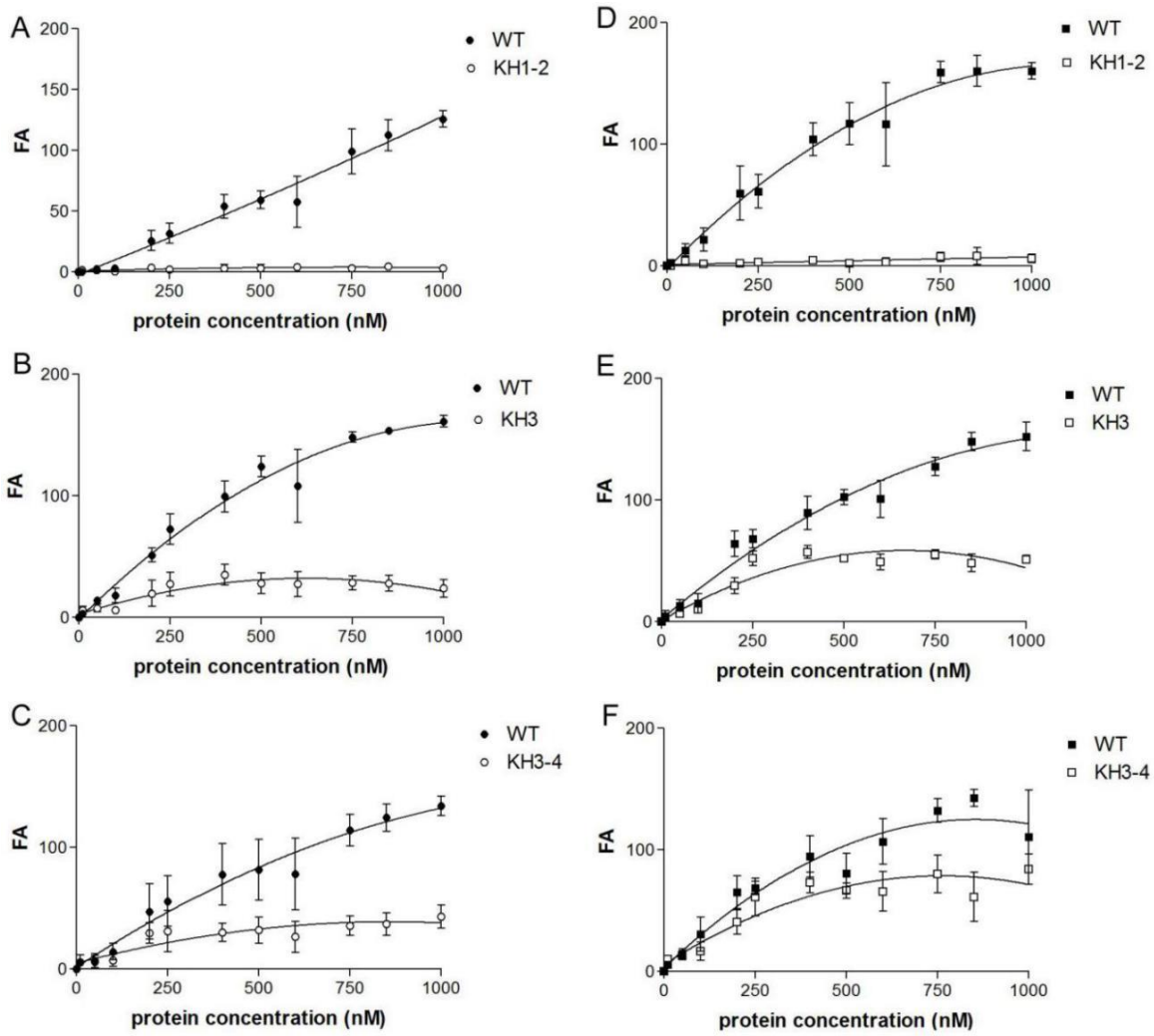

Figure 2.3 The binding profiles of WT CRD-BP and its variants with KRAS RNA (A, B, C) or CD44 RNA (D, E, F) as determined using fluorescence polarization. Ten nM of fluorescently labeled KRAS RNA or CD44 were used. Results shown were based on three separate experiments (n=3). Error bars indicate S.E.M.

The binding affinity of CRD-BP for its target RNA was affected by point mutations in the KH domains, although the effect on binding to different RNAs by each KH mutation was different (Barnes *et al*., 2015). In agreement with the *in vitro* EMSA results (Barnes *et. al.,* 2015), KH1-2 variant displayed completely abrogated binding ability for

both KRAS and CD44 RNAs, while KH3 and KH3-4 variants showed binding but relatively weaker than that of the WT CRD-BP. Overall, the FP assay displayed results which are very similar to that of EMSA (Barnes *et al*., 2015), indicating that the FP assay is a valid method for studying CRD-BP-RNA interaction.

2.3.3 Primary screening of a small molecule library

Upon establishing the FP method for studying CRD-BP-RNA interaction, I proceeded to use the FP assay to screen a small molecule library to find potential inhibitors of the CRD-BP-KRAS RNA interaction. Any decrease in fluorescence anisotropy (FA) value (fluorescence polarization units) would indicate the extent of dissociation of the KRAS RNA probe from CRD-BP, and suggests a candidate small molecule inhibitor of CRD-BP-KRAS RNA binding.

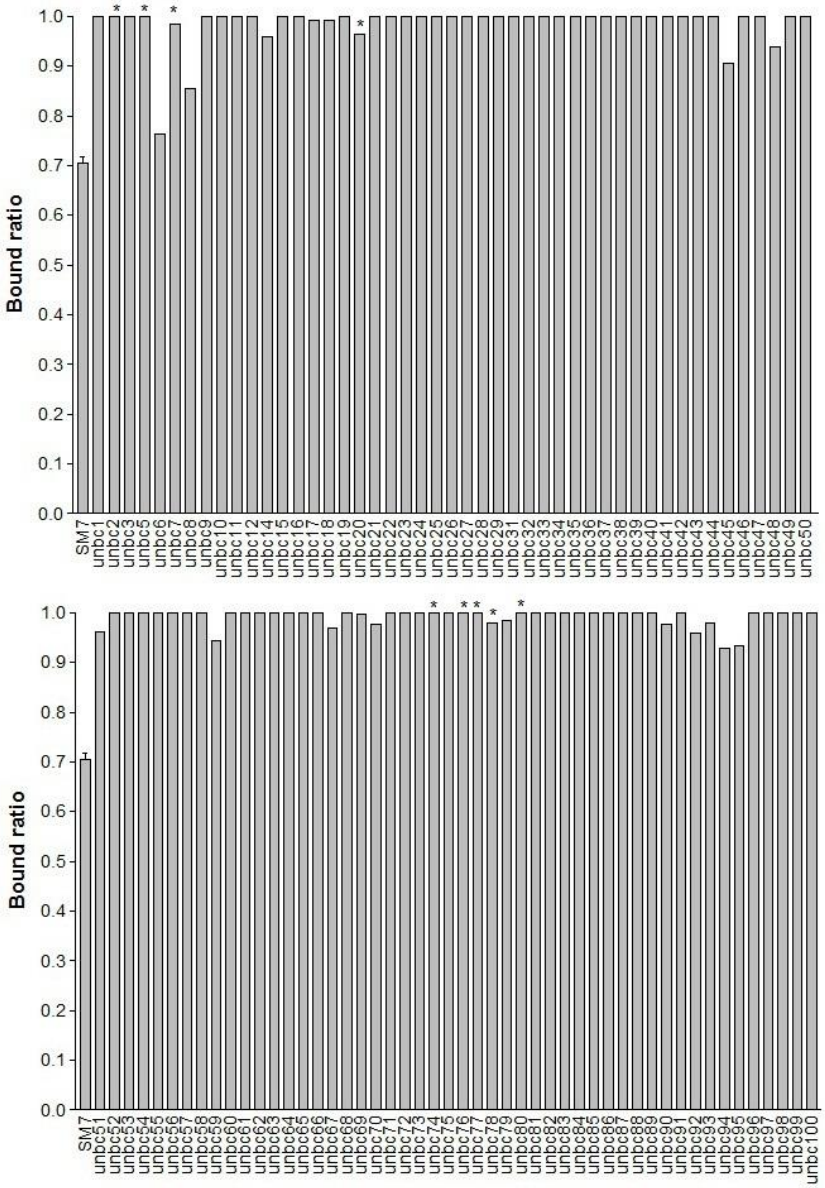

Figure 2.4 Primary screening of small molecules unbc1-100. FA value of each small molecule was compared to the DMSO control expressed as 1.0 and presented as bound ratio. Each reaction contains 0.4% DMSO. Final concentration of each small molecule was 200 μM if not indicated. Final concentration of unbc2, unbc10, unbc14 and unbc19 was 1 mM; final concentration of unbc3 was 440 μM; final concentration of unbc7 and unbc16 was 1.67 mM; final concentration of unbc9 was 910 nM; final concentration of unbc20 was 800 μM; final concentration of unbc21 and unbc24 was 1.25 mM; final concentration of unbc53 and unbc54 was 500 μM; final concentration of unbc60, unbc86 and unbc100 was 400 μM. unbc4, unbc13 and unbc30 were insoluble in DMSO and were not tested. Unbc2, unbc5, unbc7, unbc20, unbc74, unbc76-78, unbc80 were autofluorescent. Asterisk indicates autofluorescent small molecules. Ten nM of fluorescent-labeled KRAS RNA and 500 nM WT CRD-BP were used. Result shown is from one experiments (n=1), except results for SM7 were based on thirty experiments (n=30).

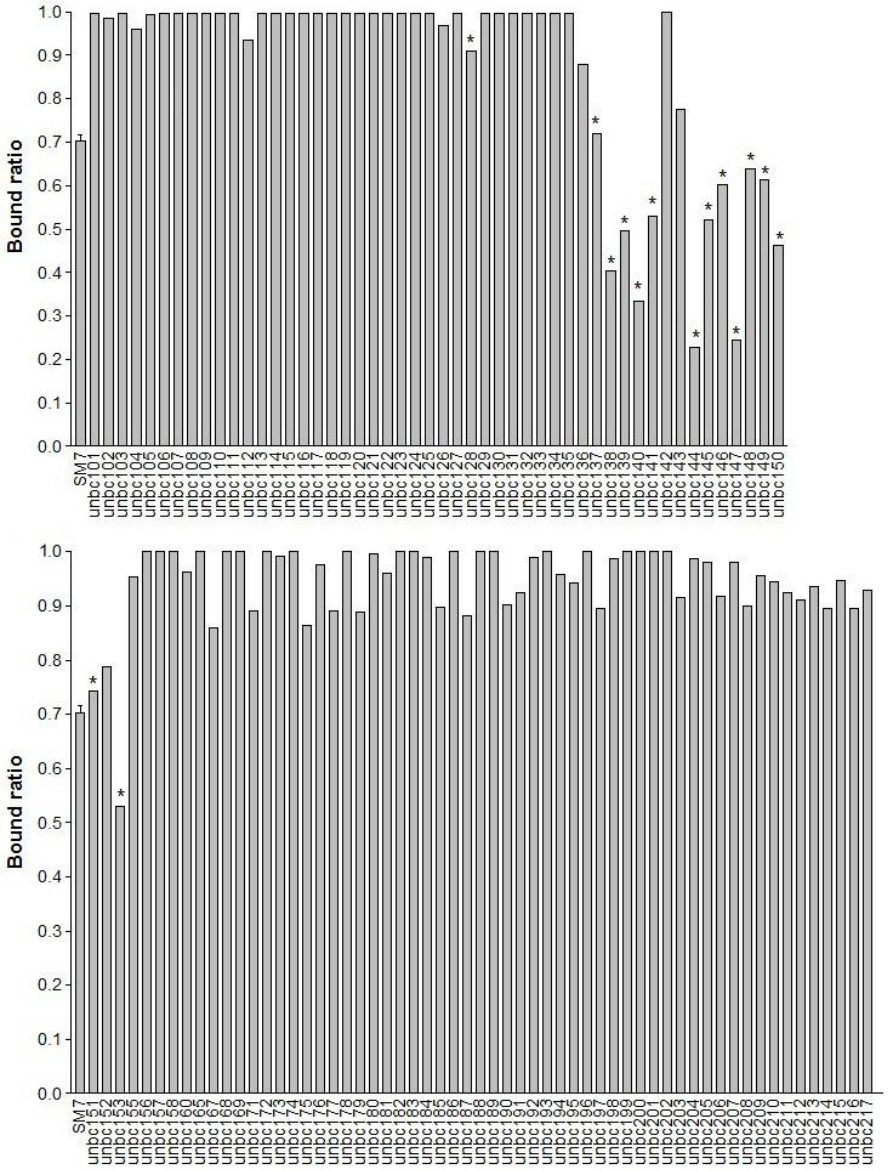

Figure 2.5 Primary screening of small molecules unbc101-217. FA value of each small molecule was compared to the DMSO control expressed as 1.0 and presented as bound ratio. One hundred μM of each small molecule was dissolved in DMSO to a final concentration of 5% DMSO. Unbc128, unbc137-141, unbc144-151, unbc153 were autofluorescent. unbc154, unbc159, unbc161-164, unbc166 were also autofluorescent and were not tested. Ten nM of fluorescent-labeled KRAS RNA and 500 nM WT CRD-BP were used. Asterisk indicates autofluorescent small molecules. Result shown is from one experiments (n=1), except results for SM7 were based on thirty experiments (n=30).

There are some compounds that have a bound ratio above 1.0. Fifty-seven compounds have a bound ratio >1.0 and ≤ 1.2, and five compounds have a bound ratio > 1.2 (data not shown). Based on the primary screening efforts, three potential candidates

were identified: unbc6, unbc143 and unbc152, whose bound ratio was less than 0.8 (Figure 2.4 and Figure 2.5). There were other small molecules which showed slight inhibitory effect (0.8 < bound ratio < 1.0), but they were not as potent as the three candidates and hence they were not studied further.

There are some autofluorescent molecules that also showing a significant reduced bound ratio (Figure 2.5). However, since the autofluorescence from these small molecules would disrupt the signal detector in FP assay, I could not tell whether the reduced bound ratio is from the inhibition effect in CRD-BP-KRAS RNA binding or not. Therefore, I would not make any conclusion for these autofluorescent small molecules in this thesis.

2.3.4 Secondary screening: dose-dependent assay of the candidate inhibitors

Dose-dependent experiments of the three candidate inhibitors were accomplished to confirm their inhibitory effect and to obtain the inhibition curve of CRD-BP-KRAS RNA binding. Concentrations of the small molecules used ranges from 0 to 100 μM.

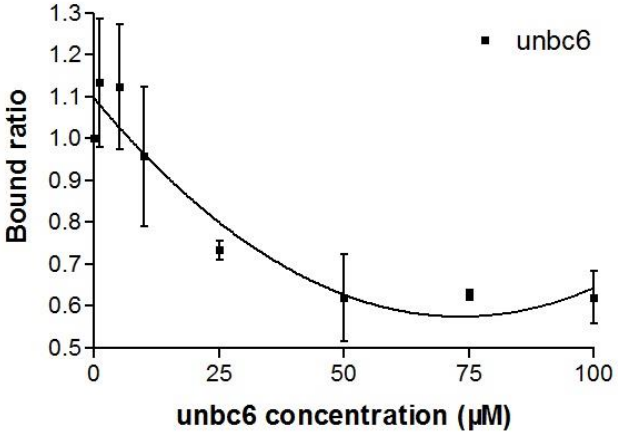

Figure 2.6 Dose-dependent FP assay of unbc6. Ten nM KRAS mRNA and 500 nM WT CRD-BP were used. Results shown were based on three separate experiments (n=3). Error bars indicate S.E.M.

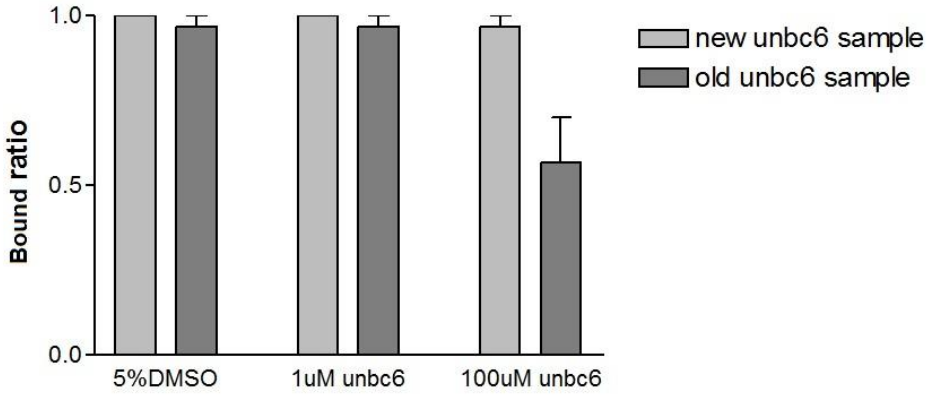

Figure 2.7 Comparing the inhibitory effects of two batches of unbc6 samples. FA values of unbc6-treated samples were normalized to those of DMSO and presented as bound ratio. Small molecules were dissolved in 5% DMSO. 10 nM KRAS mRNA and 500 nM WT were used. Results shown were based on three separate experiments (n=3). Error bars indicate S.E.M.

Initial results of unbc6 show obvious inhibitory effect in CRD-BP-KRAS RNA interaction (Figure 2.6). However, a new batch of unbc6 was not able to inhibit the CRD-BP-KRAS RNA binding (Figure 2.7). Based on the mass spectrometry analysis performed by our collaborator at the University Sains Malaysia (data not shown), the original batch of unbc6 was degraded into 6 distinct products. The inhibitory effect of unbc6 was not from the compound itself, but could be due to one of its degraded products or from the cooperation of more than one of these degraded products. Another possibility is that one or more of degraded products are autofluorescent and interfered with the FP reading. Neither the starting material nor the intermediate in unbc6 synthesis had any inhibitory effect on the CRD-BP-KRAS mRNA interaction (data not shown). Unfortunately, due to insufficient materials for further chemical analysis, the identity of the degraded products of original unbc6 remains unknown. Therefore, I focused my efforts on the other two candidate inhibitors, unbc143 and unbc152.

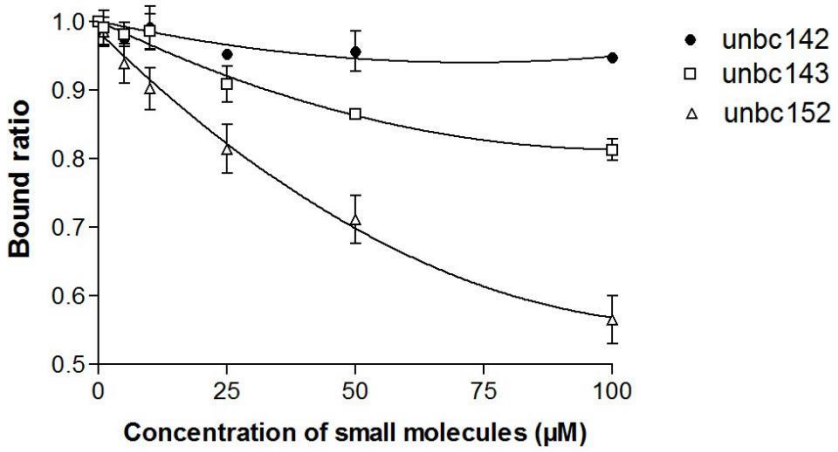

Figure 2.8 Dose-dependent FP assays of unbc143 and unbc152. Unbc142 was used as a negative control. 10 nM KRAS mRNA and 500 nM WT CRD-BP were used. Results shown were based on three separate experiments (n=3). Error bars indicate S.E.M.

As shown in Figure 2.8, new batches of unbc143 and unbc152 showed reproducible inhibitory effect on CRD-BP-KRAS RNA interaction *in vitro* based on the FP assay. Unbc143 moderately reduced the bound ratio of CRD-BP-KRAS RNA to 80% at 100 μM, while at the same concentration unbc152 suppressed bound ratio to less than 60%. In conclusion, I have successfully identified two small molecules, unbc143 and unbc152, as inhibitors of CRD-BP-KRAS RNA interaction *in vitro*.

CHAPTER 3 Assessing the inhibitors of CRD-BP-KRAS RNA interaction on KRAS gene expression in colon cancer cells

At the outset of this research using the method of chemical cross-linking coupled to immunoprecipitation, it was previously demonstrated that CRD-BP can physically interact with KRAS mRNA at both the coding region and 3'UTR (Mongroo *et al.*, 2011). The authors further showed that knockdown of CRD-BP in SW480 colon cancer cells led to decreased KRAS protein expression, while over-expression of CRD-BP led to increased KRAS protein expression in LIM2405 colon cancer cells (Mongroo *et al.*, 2011). The concomitant changes in CRD-BP and KRAS protein expression suggest that CRD-BP can control the expression of KRAS in colon cancer cells. It was postulated that CRD-BP binds to KRAS mRNA to protect the transcript from rapid decay thereby leading to increased KRAS protein levels.

Dr. Lee's lab has recently shown that antisense oligonucleotides (AONs) SM7 and SM6 were effective inhibitors of CRD-BP-KRAS mRNA interaction *in vitr*o (Sebastian Mackedenski, unpublished observations). In Chapter 2 of this thesis, I successfully used fluorescence polarization method to identify two small molecules, unbc143 and unbc152, which were capable of inhibiting CRD-BP-KRAS mRNA interaction. In this Chapter, I used quantitative real-time polymerase chain reaction (qRT-PCR) and Western blot analysis to assess the effect of 2'-O-methyl version of SM6 and SM7 antisense oligonucleotides, as well as unbc143 and 152, for their abilities to influence KRAS RNA

gene expression in three human colon cancer cells.

3.1 Methodology – Detecting CRD-BP and KRAS mRNA levels in cells

Using the qRT-PCR method, I first treated SW480 colon cancer cells with CRD-BP siRNAs (Table 3.1) to determine if CRD-BP can truly influence KRAS expression. After the successful establishment of the relationship between CRD-BP and KRAS in SW480 cells, I then assessed the effect of SM6, SM7, unbc143 and unbc152 on gene expression in the cells. For the AON SM6 and SM7 experiments, I used SM2, the AON that did not have inhibitory effect on CRD-BP-KRAS mRNA interaction *in vitro* as the negative control. All the AONs were assessed at a concentration previously shown to be effective in inhibiting gene expression (King *et. al.*, 2014). Small molecule candidates, unbc143 and unbc152, were assessed using 3 different concentrations.

Table 3.1 Sequences of CRD-BP siRNAs

CRD-BP siRNAs	Duplex sequences	References
CRD-BP siRNA1	5'-CCU GGC UGC UGU AGG UCU UUU CC-3' 3'-GGA CCG ACG ACA UCC AGA AAA GG-5'	Ioannidis *et. al.,* 2005
CRD-BP siRNA2	5'-GGA GGA GAA CUU CUU UGG UCC CAA G-3' 3'UU CCU CCU CUU GAA GAA ACC AGG GUU C-5'	Kato *et. al.,* 2007

3.1.1 Cell preparation and total RNA extraction

Colon cancer cell line SW480, HT29 and CaCO2 (all from American Type Culture Collection, Virginia, USA) were stored in liquid nitrogen medium containing 5% DMSO. Cells were rapidly thawed in 37°C water bath for 2 minutes. Cells were transferred into a 25 cm^2 tissue culture flask and top up to 10 mL with the medium EMEM (BioWhittaker,

Cologne, Germany). Cells were cultured in the direct heat CO_2 incubator (37°C, 5% CO_2) until 90% confluent, and then were split into two to four 75 cm^2 tissue culture flasks. When cells were 90% confluent, cells were first washed with 3 mL of PBS (BioWhittaker, Cologne, Germany) before trypsinization using 2 mL 0.25% trypsin-EDTA in 37 °C incubator for 2-5 minutes. After all the cells were detached from the culture flask, trypsin was inactivated with 18 mL EMEM (with 10% serum). Twenty μL resuspended cells were then mixed with 20 μL of trypan blue prior cell counting using the Bright-Line Hemacytometer (Hausser Scientific, Pennsylvania, USA). Cells were plated onto 6-well plates with a cell density of 150,000 cells/well (for CRD-BP siRNA and AON experiments) or 300,000 cells/well (for small molecule experiments), depending on the type of experiments. After 24 hours incubation, cells were treated with test agents (CRD-BP siRNA, AON or small molecules).

In CRD-BP siRNA transfection, cells were transfected with CRD-BP siRNA1 (40 nM), CRD-BP siRNA2 (40 nM) and scramble negative control (SN) (40 nM). SN is a double stranded RNA with scramble sequence. For each well in a 6-well plate, 4 μL lipofectamine 2000 transfection reagent (Invitrogen, California, USA) was diluted with Opti-MEM to make mixture A (total volume 250 μL). To make mixture B (total volume of 250 uL), CRD-BP siRNA1, CRD-BP siRNA2 or SN was diluted with Opti-MEM. The mixtures were incubated at room temperature for 5 minutes. Then, mixture A and B were mixed vigorously, followed by a 20-minute incubation at room temperature. To cells which had media renewal (2 mL media/well), 500 μL of the nucleic acid-lipid complexes

were added. Cells were transfected again 48 hours after the first transfection using the same conditions. Forty-eight hours after the second transfection, cells were harvested as described below.

In AON transfection, cells were transfected with antisense oligonucleotides SM2 (125 nM), SM6 (125 nM) and SM7 (125 nM). For each well in a 6-well plate, 4 μL lipofectamine 2000 transfection reagent (Invitrogen, California, USA) was diluted with Opti-MEM to make mixture A (total volume 250 μL).SM2, SM6, or SM7 was diluted with Opti-MEM to make mixture B (total volume 250 μL). The following steps were the same as described in CRD-BP siRNA transfection above.

In experiments with small molecules, cells were treated with unbc143 (1 μM, 10 μM, 20 μM in a final concentration of 2% DMSO), unbc152 (1 μM, 10 μM, 20 μM in a final concentration of 2% DMSO) or mock control (2% DMSO). Small molecules were first diluted to each concentration with fresh medium. Then, old medium was replaced with fresh medium containing small molecules. Forty-eight hours after treatment with the small molecules, cells were harvested as described below.

The reagents for RNA extraction were supplied by the *mir*Vana miRNA isolation kit (Invitrogen, California, USA). The protocol used was according to the manufacturer's instructions except for the elution step at the end; cells were rinsed twice with 2 mL PBS prior to addition of 200 μL lysis buffer to each well. Lysate was pooled from 2 wells (400 μL) in a 1.5 mL microcentrifuge tube and was mixed with 40 μL homogenate additive followed by incubation on ice bath for 10 minutes. After that, 400 μL of

phenol-chloroform were added to lysate, and the mixture was vortexed to mix for 30 seconds before centrifugation at 10,000 x g for 5 minutes at room temperature. The upper phase of the mixture was collected and mixed with 1.25 x 100 % ethanol (room temperature). The mixture was mixed well and then loaded into a filter column (maximum loading volume 700 μL prior to spinning at 10,000 x g for 15 seconds. The flow-through liquid was discarded before 700 μL Wash Solution 1 was added into the filter column. Column was washed twice with 500 μL Wash Solution 2/3 by 10,000 x g spinning for 15 seconds after flow-through liquid from last wash was disposed. To get rid of all the wash solution, column was spun for 1 minute with the same spinning rate before elution of RNA. Boiling (95°C) nuclease-free water was used to elute the RNAs from the column. The collected RNAs were then quantified using NanoDrop 1000 spectrophotometer (Thermo Scientific, Illinois, USA).

3.1.2 cDNA synthesis and Quantitative Real-time Polymerase Chain Reaction (qRT-PCR)

Before cDNA synthesis, I first removed any genomic DNAs from the cell lysate using DNase treatment & removal kit (Life Technologies, California, USA). cDNAs were then synthesized using iScript cDNA synthesis kit (Bio-Rad Laboratories, California, USA) as according to the instructions provided in the kit: 1 μg of total RNA was mixed with 1 μL of 10 x DNase I buffer, 1 μL of DNase I and top up to 10 μL with nuclease-free water. After 37°C dry bath for 30 minutes, reaction was stopped by adding 2 μL of DNase inactivation reagent. Mixture was then incubated at room temperature for 2 minutes and

spun at 10,000 x g for 1.5 minutes. Ten µL of the supernatant was collected and mixed it with 4 µL of 5 x iScript reaction mix, 1 µL of iScript reverse transcriptase and 5 µL of nuclease-free water. Mixture was then placed in the thermocycler and cDNAs were synthesized using the following program:

25 °C	5 min
42°C	30 min
85°C	5 min
4°C	Indefinite

Except for the 1 µL cDNA, the other reaction reagents (Tables 3.3, 3.4 and 3.5) were first mixed as a master mix and added after the cDNA was loaded into each well on the 96-well PCR plate (Axygen, California, USA). Sequences of primers and probes required for qRT-PCR are listed in Table 3.2. These primers and probes were purchased from Integrated DNA Technologies, Iowa, USA.

Table 3.2 Sequences of primers and probes

Primers or probes		Sequences	References
CRD-BP primer	forward	5'-AAC CCT GAG AGG ACC ATC ACT-3'	Kato *et. al.,* 2007
CRD-BP primer	reverse	5'-AGC TGG GAA AAG ACC TAC AGC-3'	
CRD-BP probe	Taqman	5'/56-FAM/-TGT TGC AGG GCC GAG CAG GA/3BHQ_1/-3'	
KRAS primer	forward	5'-CGA ATA TGA TCC AAC AAT AGA G-3'	Cogoi *et. al.,* 2013
KRAS primer	reverse	5'-ATG TAC TGG TCC CTC ATT-3'	
KRAS probe	Taqman	5'/56-FAM/-TAC TCC TCT TGA CCT GCT GTG/3BHQ_1/-3'	
β-actin primer	forward	5'-TTG CCG ACA GGA TGC AGA AGG A-3	Mehmood *et. al.,* 2016
β-actin primer	reverse	5'-AGG TGG ACA GCG AGG CCA GGA T-3'	

Table 3.3 Reagents for CRD-BP qPCR

Reaction reagents (for TaqMan assay)	Concentration/ volume
CRD-BP forward primer	400 nM
CRD-BP reverse primer	400 nM
CRD-BP probe	200 nM
IQ SuperMix	12.5 μL
cDNA	1 μg
Nuclease-free water	Top up to 25 μL

Table 3.4 Reagents for KRAS qPCR

Reaction reagents (for TaqMan assay)	Concentration/ volume
KRAS forward primer	200 nM
KRAS reverse primer	200 nM
KRAS probe	100 nM
IQ SuperMix	12.5 μL
cDNA	1 μg
Nuclease-free water	Top up to 25 μL

Table 3.5 Reagents for in β-actin qPCR

Reaction reagents (for SybrGreen assay)	Concentration/ volume
β-actin forward primer	200 nM
β-actin reverse primer	200 nM
IQ SYBRGreen SuperMix	12.5 μL
cDNA	1 μg
Nuclease-free water	Top up to 25 μL

Technical triplicates were performed for each reaction. Tubes with no template and tubes with no reverse transcriptase were used as controls. After all the reagents were added, the 96-well PCR plates were sealed properly, and then ran using their designated protocols (see below) in the Multicolor PCR detection system (Bio-Rad, California, USA). β-Actin was used as a reference gene.

qPCR cycle for CRD-BP is:

95 °C		2 min
95 °C	40 X	45 sec
53 °C		30 sec

qPCR cycle for KRAS is:

95 °C		3 min
95 °C 58 °C	} 40 X	10 sec 30 sec

qPCR cycle for β-actin is:

95 °C		3 min
95 °C 60 °C	} 40 X	10 sec 30 sec

Melt curve analysis was performed to assess β-actin qPCR product specificity. Temperature increased from 60°C by 0.5°C increments to 95°C; each increment lasted for 30 seconds.

The cycle number at which the exponentially accumulated amplified product give a detectable fluorescent signal is called threshold cycle (C_T). Each cycle would yield two-fold increased amplified products. C_T of the three replicates are averaged first, and the be analyzed using following method:

First, the C_T of the target gene (i.e. KRAS) is normalized to that of the reference gene (i.e. β-actin), for both the test sample (i.e. CRD-BP siRNA1 transfected sample) and the calibrator sample (i.e. SN transfected sample):

$$\Delta C_{T\,(test)} = C_{T\,(target,\,test)} - C_{T\,(reference,\,test)}$$

$$\Delta C_{T\,(calibrator)} = C_{T\,(target,\,calibrator)} - C_{T\,(reference,\,calibrator)}$$

Then, the C_T of the test sample is normalized to the C_T of the calibrator sample:

$$\Delta\Delta C_T = \Delta C_{T\,(test)} - \Delta C_{T(calibrator)}$$

Finally, the expression ratio is calculated:

Normalized expression ratio = $2^{-\Delta\Delta CT}$

3.2 Methodology – Detecting CRD-BP and KRAS protein levels in cells

According to the results by Mongroo *et. al.,* (2011), CRD-BP knocked down leads to down-regulation of KRAS protein expression in SW480 colon cancer cells. Therefore, the first step of my experiment was to confirm their results.

3.2.1 Cell preparation and protein extraction

Please refer to the cell preparation steps described in section 3.1.1.

When cells were ready for harvesting, they were first washed twice with 2 mL PBS. One hundred fifty μL of lysis buffer (see Table 3.6) were then added to each well, and cell lysates from two wells were combined into an Eppendorf tube. Three hundred μL of cell lysates in each tube were mixed with 1.2 mL of 100% acetone and the mixture were then stored in the -20°C fridge overnight.

Table 3.6 Reagents used for protein lysis buffer

Protein lysis buffer	Volume
5M NaCl	1.2 mL
1M Tris-Cl	2 mL
10% Triton X-100	4 mL
10% SDS	2 mL
Water	30.8 mL
Sterile filtered (0.2 μM) and stored in 4°C	

On the following day, the mixtures were centrifuged at 16,000 x g for 10 minutes in the cold room. The acetone was carefully discarded and the precipitate dried in the fume hood for 10 minutes. Twenty μL of water was used to resuspend the precipitate in each tube. However, the volume of water for dissolving proteins depends on the cell density. If cell density was low at the time of harvesting, then the volume of water for pellet

resuspension will be reduced. Tubes from the same treated sample were combined and spun at 10,000 x g for 2 minutes at room temperature. Supernatants were collected, and 1 μL of supernatant was diluted with 9 μL of water and subjected to protein quantification using the Pierce BCA protein assay kit (Thermo Scientific, Illinois, USA).

3.2.2 Western blot analysis

Please refer to section 2.1.1 for the description of protein quantification. After protein concentration was determined, they were ready for Western blot analysis.

Western blot analysis consists of three steps: polyacrylamide gel electrophoresis, membrane transferring and immunostaining. The reagents used for SDS-PAGE are shown in Table 2.2. Twelve μL of protein (15-30 μg) was mixed with 3 μL 5 x SDS buffer (with 5% β-mercaptoethanol), and then boiled for 10 minutes. Sample proteins and protein marker were loaded and the gel was run at 160 voltages for 45 minutes.

After the gel electrophoresis was done, proteins were transferred from the gel to the Amersham Protran Premium 0.45 μm nitrocellulose blotting membrane (GE Healthcare Life Sciences, Buckinghamshire, UK). Transferring was performed at 100 voltages for 1 hour in the cold room. Since proteins would migrate from the negative charge to the positive charge, they would attach to the membrane by placing the gel-membrane sandwich at a designated electrode direction. The membrane with transferred proteins was then blocked with 20 mL of 1x TBST (0.05 M Tris-Cl, 0.03 M NaCl, 0.1% tween 20, pH 7.4) with 5% skim milk (or 5% BSA, depending on antibody type) on a waver in the cold room overnight. Skim milk (or BSA) would attach to the membrane at where no protein

binds to, and reduces non-specific binding resulting in reduced background signal in immunostaining.

The next day, membrane was rinsed twice with 1x TBST prior to incubation with primary antibodies. Since several target proteins were to be detected, the membrane was cut into 2-3 pieces as according to the target protein sizes. Antibodies were first diluted in optimized concentrations (see Table 3.7) with 1 x TBST containing 1% skim milk (or 5% BSA, depending on antibody type). Then, membranes were incubated with primary antibodies on a waver in room temperature for 1 hour (or overnight, depending on antibody type) followed by 10-minute washing with 1x TBST for 3 times. After that, membranes were incubated with secondary antibodies (see Table 3.7) for 1 hour in room temperature on a waver prior to 10-minute washing with 1x TBST 3 times. Reagents from the SuperSignal West Pico Chemiluminescent Substrate kit (or SuperSignal West Femto Maximum Sensitivity Substrate kit when antibody signal intensity is weak) (Thermo Scientific, Illinois, USA) were warmed to room temperature before use. The 3 mL of each substrate components from the kit were mixed prior to adding to the membranes. After 5 minute incubation, membranes were visualized using the FluorChem Q system (Proteinsimple, California, USA) and analyzed by AlphaView Q software (ProteinSimple, California, USA). β-Actin, GAPDH and thioredoxin were used as reference genes.

Table 3.7 Dilutions of primary antibodies and secondary antibodies

Primary antibody		Corresponding Secondary antibody	
IMP-1	1:1000	Goat anti-mouse IgM-HRP	1:4000
K-Ras	1:500	Anti-mouse IgG-HRP	1:4000
β-Actin	1:4000	Anti-mouse IgG-HRP	1:4000
GAPDH	1:20000	Anti-mouse IgG-HRP	1:4000
Thioredoxin	1:1000	Anti-rabbit IgG-HRP	1:2000
Phospho-MAPK	1:1000	Anti-rabbit IgG-HRP	1:2000
Phospho-Akt	1:2000	Anti-rabbit IgG-HRP	1:2000

IMP1 (D-9; sc-166344), K-Ras (F234; sc-30) and goat anti-mouse IgM-HRP (sc-2064) were purchased from Santa Cruz Biotechnology, Texas, USA. Monoclonal anti-β-Actin (clone AC-15) and monoclonal anti-GAPDH (clone GAPDH-71.1) were purchased from Sigma-Aldrich, Missouri, USA. Anti-thioredoxin/TRX antibody ab26320 was purchased from Abcam, Cambridge, UK. Phospho-p44/42-MAPK (Erk1/2) (Thr202/Tyr204) antibody and phospho-Akt (Ser473) (D9E) XP rabbit mAb were purchased from Cell Signaling Technology, Massachusetts, USA. Anti-mouse IgG-HRP conjugate and anti-rabbit IgG-HRP conjugate were purchased form Promega, Wisconsin, USA.

To quantify the protein expression, several steps are required:

The luminescence intensity (I) of the target protein (i.e. KRAS) was first normalized to that of the reference protein (i.e. β–actin), for both the test sample (i.e. CRD-BP siRNA1 transfected sample) and the calibrator sample (i.e. SN transfected sample).

$$\text{Expression}_{(\text{test})} = I_{(\text{target, test})} / I_{(\text{reference, test})}$$

$$\text{Expression}_{(\text{calibrator})} = I_{(\text{target, calibrator})} / I_{(\text{reference, calibrator})}$$

Then, the expression ratio of the target protein is calculated by normalizing the

protein expression of the test sample to that of the calibrator sample:

$$\text{Expression ratio} = \text{Expression}_{(\text{test})} / \text{Expression}_{(\text{calibrator})}$$

Normalized data obtained from qPCR (Section 3.1.2) and Western blot analyses were then plotted and statistically analyzed using GraphPad Prism Software. A paired T-test with two-tailed distribution was used to analyze the significance of the data. The Excel Software was used for the T-test. In the T-test function, the normalized data of all the replicates of the test sample (i.e. CRD-BP siRNA treated sample) are entered in Array1, and the normalized data of all the replicates of the calibrator sample (i.e. SN transfected sample) are entered in Array2. P-value was then be calculated. If P-value $\leq$ 0.05, data would be considered as statistically significant.

3.3 Results and Discussion

3.3.1 mRNA and protein expression of CRD-BP and KRAS in CRD-BP-knocked down colon cancer cells

The purpose of this section is to understand the relationship between CRD-BP and KRAS at the post-transcriptional and post-translational levels. By comparing their gene expressions, we can test the hypothesis on how CRD-BP regulates KRAS and what kind of modulation mechanism might exist. As mentioned earlier, I hypothesize that CRD-BP might compete with translational repressor(s) in binding to KRAS mRNA. To test this hypothesis and to determine whether the relationship between CRD-BP and KRAS mRNA exists, I used two specific siRNA against CRD-BP to knockdown CRD-BP mRNA levels and measured the expression of KRAS mRNA and protein levels. Both the

mRNA and protein levels of CRD-BP and KRAS were assessed in SW480 and CaCO2 colon cancer cells transfection with the two siRNAs (Table 3.1). If my hypothesis is true, knockdown of CRD-BP should repress KRAS translation without affecting KRAS RNA level.

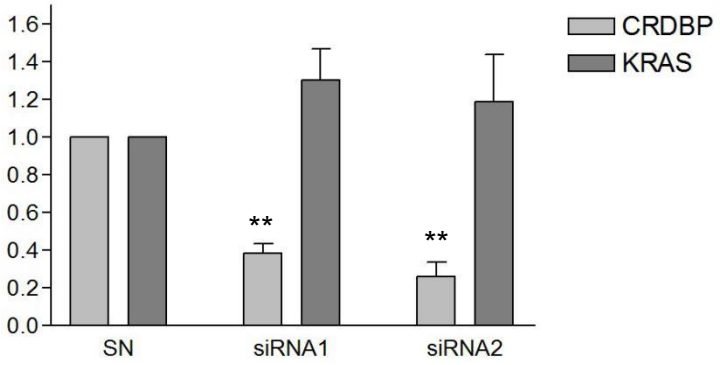

Figure 3.1 CRD-BP and KRAS mRNA expression in CRD-BP-knocked down SW480 cells. SW480 colon cancer cells were transfected with siRNA1, siRNA2, or scrambled-negative (SN) as described in section 3.1.1. Results were normalized to mRNA level of β–actin and then expressed relative to the SN as shown. Results shown were based on four separate biological replicates (n=4). Error bars indicate S.E.M. *P < 0.05, **P < 0.01.

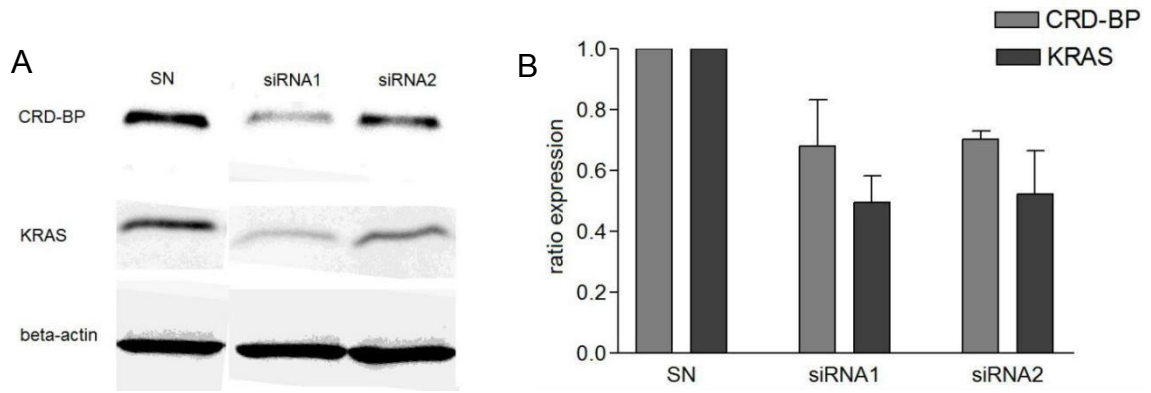

Figure 3.2 CRD-BP and KRAS protein expression upon CRD-BP-knocked down in SW480 colon cancer cells. (A) SW480 cells were transfected with siRNA1, siRNA2, or scrambled-negative (SN) as described in section 3.3.1. Cell lysates collected were subjected to Western blot analysis as shown. The result shown is a representative from two biological replicates. (B) The levels of CRD-BP and KRAS protein levels in siRNA1- and siRNA2-transfected cells were normalized to that of β–actin and then expressed relative to the SN as shown. Results shown are the average data from (A) and another separate biological replicate (n=2). Error bars indicate S.E.M.

Mongroo *et. al*. (2011) showed that upon knockdown of CRD-BP (decreased of 75%)

in SW480 cells using a specific siRNA against CRD-BP mRNA, there was approximately 60% decreased in KRAS protein level. However, the authors did not report any changes in mRNA levels of CRD-BP and KRAS (Mongroo *et. al.,* 2011). Using two different siRNAs against CRD-BP, I found that no significant change in the KRAS mRNA levels was observed upon the knockdown of CRD-BP (Figure 3.1). However, knockdown of CRD-BP (protein and mRNA levels) led to 50% decreased in KRAS protein levels (Figure 3.2), which is in good agreement with the results by Mongroo *et. al.* (2011). These results imply that CRD-BP most likely influences KRAS expression at the level of translational control. It agrees with the hypothesize that CRD-BP competes with KRAS translation repressor(s) for binding to the KRAS transcript. The CRD-BP commonly holds and protects KRAS transcripts and allows them to process to translation. However, in cases where there is a reduced level of CRD-BP leading to a reduced amount of CRD-BP bound to KRAS transcript (for instance in CRD-BP-knocked down cells), translation repressor(s) (such as let-7 microRNA family) would be free to bind to KRAS mRNA and suppress its translation leading to less amount of KRAS proteins. The KRAS gene is one of the targets of tumor suppressor microRNA let-7. Since both CRD-BP and let-7 can target the 3'UTR of KRAS mRNA, CRD-BP might prevent let-7 binding to KRAS mRNA and leading to translation repression (Johnson *et. al.*, 2005; Bell *et. al.*, 2013).

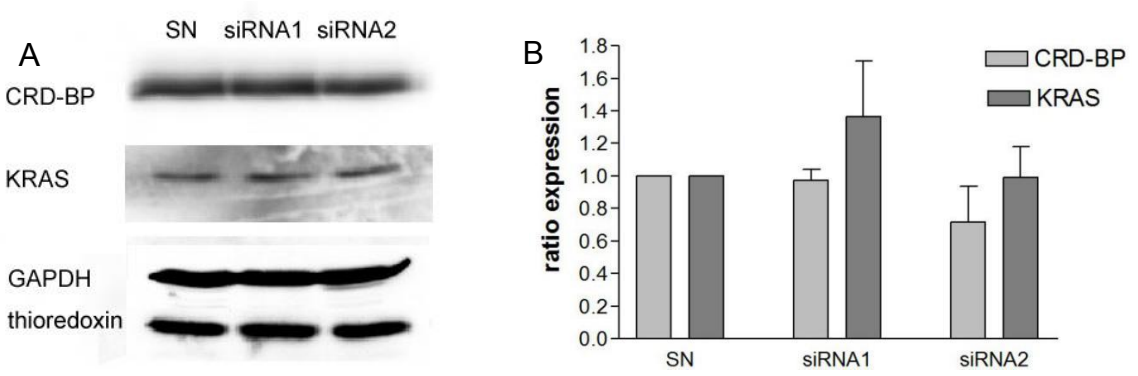

Figure 3.3 CRD-BP and KRAS protein expression upon CRD-BP-knocked down in CaCO2 cells. (A) CaCO2 colon cancer cells were transfected with siRNA1, siRNA2, or scrambled-negative (SN) as described in section 3.3.1. Cell lysates collected were subjected to Western blot analysis as shown. The result shown is a representative from two biological replicates. (B) The levels of CRD-BP and KRAS protein levels in siRNA1- and siRNA2-transfected cells were normalized to that of thioredoxin and then expressed relative to the SN as shown. Results shown are the average data from (A) and another biological replicate (n=2). Error bars indicate S.E.M.

To simply assess effect of CRD-BP siRNAs on the KRAS protein levels in the other colon cancer cell lines, I conducted the same transfection and Western blot analysis in CaCO2 cells. In contrast to SW480 cells, there was no significant decrease in both CRD-BP and KRAS protein levels in CaCO2 cells upon treatment with siRNAs against CRD-BP (Figure 3.3). According to the report by Mongroo *et. al.* (2011), CRD-BP mRNA levels was around 13-fold higher in CaCO2 cells than SW480 cells. Therefore, it is possible that the abundant CRD-BP present in CaCO2 cells could be masking the effect of the siRNAs and hence no visible knockdown of CRD-BP was observed in CaCO2 cells. Such results showed that CaCO2 cells are less susceptible to siRNAs against CRD-BP.

3.3.2 Effect of AON on CRD-BP and KRAS gene expression

After establishing the relationship between CRD-BP and KRAS mRNA in SW480 cells, the next step was to assess the AON candidate inhibitors on the cells. SM6 and SM7

were shown to block the binding of CRD-BP to KRAS RNA to 50% at 4.72 nM and 1.18 nM respectively in an EMSA (Sebastian Mackedenski, unpublished data). I first measured the mRNA levels of CRD-BP and KRAS in SW480 cells using qRT-PCR. Then, the Western blot analysis was performed on both SW480 and CaCO2 colon cancer cell lines to assess the protein levels of CRD-BP and KRAS. The AONs were expected to bind to KRAS mRNA at the binding site of CRD-BP on KRAS mRNA. Without the binding of CRD-BP, a hypothetical translational repressor could bind to KRAS mRNA and block translation. If SM6 and SM7 bind to KRAS mRNA in cells, a decline in KRAS protein expression is expected.

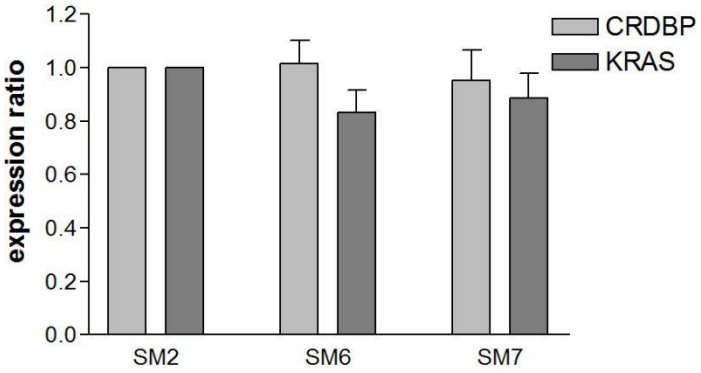

Figure 3.4 CRD-BP and KRAS mRNA expression in SW480 cells transfected with AONs. SW480 colon cancer cells were transfected with SM2, SM6, or SM7 as described in section 3.1.1. Results were normalized to mRNA level of β–actin and then expressed relative to the SM2 as shown. Results shown were based on four separate biological replicates (n=4). Error bars indicate S.E.M.

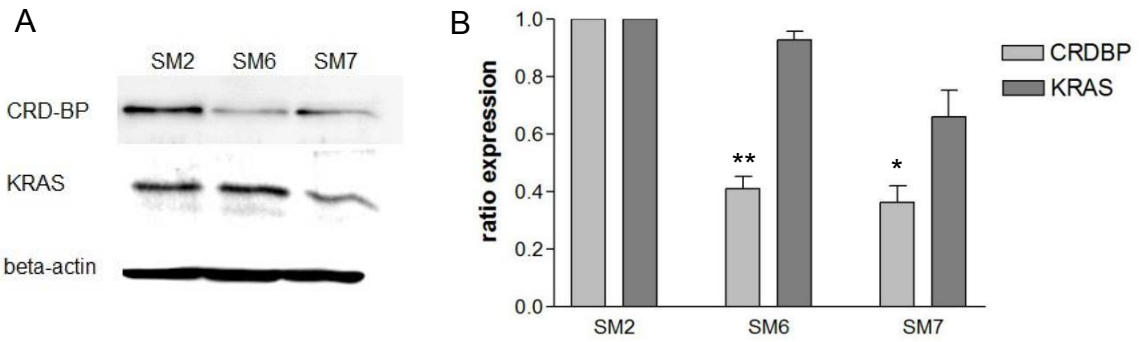

Figure 3.5 CRD-BP and KRAS protein expression in SW480 cells transfected with AONs. (A) SW480 colon cancer cells were transfected with SM2, SM6, or SM7 as described in section 3.1.1. Cell lysates collected were subjected to Western blot analysis as shown. The result shown is a representative of four biological replicates (n=4). (B) The levels of CRD-BP and KRAS protein levels in SM6- and SM7-transfected cells were normalized to that of β–actin and then expressed relative to the SM2 as shown. Results shown were based on (A) and three other biological replicates (n=4). Error bars indicate S.E.M. *P < 0.05, **P < 0.01.

Because DNA sequences are more stable for long-term storage and more economical to generate, the antisense oligonucleotides were made as deoxyribonucleotides for *in vitro* EMSA and FP experiments. However, single stranded RNA bases have higher affinity than single stranded DNA bases in cells and *in vitro*. Therefore, we decided to generate these antisense oligonucleotides as more stable 2'O-methylated version of RNA bases for cell-based experiments. Since the RNase H cleaves only DNA-RNA hybrids and should not degrade the AON-KRAS RNA complex, it is expected that KRAS RNA level kept stable after cells were transfected with AONs (Figure 3.4).

As is shown in Figure 3.5, antisense oligonucleotides SM6 and SM7, which were designed against KRAS transcript, significantly decreased CRD-BP levels. However, no obvious KRAS inhibitory effect was seen with SM6 and SM7. Since the AONs inhibitors are likely to interact with KRAS mRNA thereby occluding KRAS mRNA-bound CRD-BP leading to the accumulation of CRD-BP, it is possible that AONs inhibitors

might regulate CRD-BP through disrupting the expression of other CRD-BP targeted genes. For example, β-catenin can promote CRD-BP transcription through binding to CRD-BP promoter (Gu *et. al.*, 2008). Two of the CRD-BP direct targets, βTrCP1 and IGF2 mRNA, however, are involved in the modulation of β-catenin, implying the feedback regulation of CRD-BP (Noubissi *et. al.*, 2006; Djiogue *et. al.*, 2013). When more CRD-BP binds to these mRNAs, up-regulation of βTrCP1 and down-regulation of IGF2 inactivate β-catenin, resulting in suppression CRD-BP promoter-driven transcription.

The sequences of SM6 and SM7 cover the two tandem stem-loops of KRAS transcript, which is considered as the minimum binding region of CRD-BP. When SM6 and SM7 hybridize with KRAS mRNA, they might take the place of CRD-BP to compete with translation repressor(s) at the same binding region on KRAS mRNA, and therefore still inhibit translation repression.

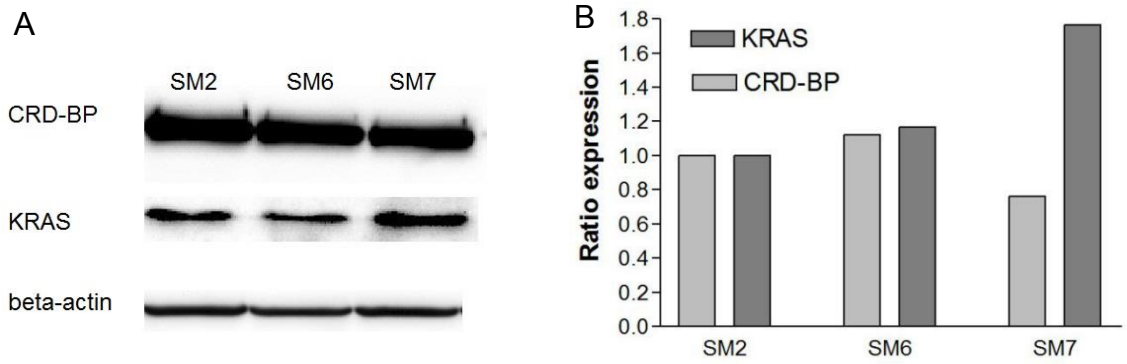

Figure 3.6 CRD-BP and KRAS protein expression in CaCO2 cells transfected with AONs. (A) CaCO2 colon cancer cells were transfected with SM2, SM6, or SM7 as described in section 3.1.1. Cell lysates collected were subjected to Western blot analysis as shown. The result shown is from one biological replicate. (B) The levels of CRD-BP and KRAS protein levels in SM6- and SM7-transfected cells quantified from (A) were normalized to that of β–actin and then expressed relative to the SM2 as shown. The results shown is one biological replicate (n=1).

To determine whether AONs SM6 and SM7 have similar inhibitory effect on other colon cancer cell line, I performed similar experiments on CaCO2 cell line. My preliminary results showed that although SW480 and CaCO2 are both colorectal cancer cells, no obvious inhibition on CRD-BP expression was observed in CaCO2 (Figure 3.6). Both SW480 and CaCO2 are colon cancer cell lines, but their responses to the AON inhibitors were different. As shown in Figure 3.3, CaCO2 was insensitive to CRD-BP silencing and the similar reasons may account for why CaCO2 cells were irresponsive to the AONs.

3.3.3 Effect of small molecules, unbc143 and unbc152, on CRD-BP and KRAS gene expression

According to the results from fluorescence polarization experiments (Figure 2.8), the small molecule candidates, unbc143 and unbc152, were able to decrease CRD-BP-KRAS RNA binding by about 20% and 40% respectively. Therefore, it will be interesting to see if both unbc143 and unbc152 have any effect on KRAS expression in SW480 colon cancer cells where the relationship between CRD-BP and KRAS mRNA exists. RT-qPCR analysis was conducted in SW480 colon cancer cells and Western blot analysis was conducted in both SW480 and HT29 colon cancer cells. In contrast to AONs, small molecules might act in a different way in blocking the CRD-BP-KRAS mRNA interaction. Since proteins are tend to recognize the structure of molecules while RNAs are tend to recognize the sequence, I hypothesize that the small molecules displaying complex structures are likely to bind CRD-BP protein rather than KRAS mRNA. If this is

true, then KRAS mRNA would be bound by translation repressor(s) and translation would be blocked.

Lastly, to investigate whether the unbc152 inhibitory effect on KRAS expression would suppress the KRAS downstream signaling pathways, I carried out Western blot analysis using cell lysates from SW480 cells treated with the small molecule and examine the expression of phospho-Akt and phospho-MAPK, which are phosphorylated and activated by KRAS signaling. If KRAS activity was inhibited by the small molecule, then both phospho-Akt and phospho-MAPK expression are expected to be suppressed.

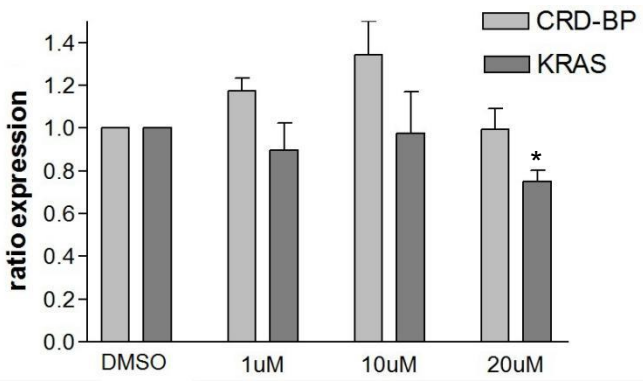

Figure 3.7.CRD-BP and KRAS mRNA expression in unbc143-treated SW480 cells. SW480 colon cancer cells were treated with three different concentrations (1, 10, 20 μM) of unbc143 as described in section 3.1.1. Results were normalized to mRNA level of β–actin and then expressed relative to DMSO-treated control as shown. Results shown were based on four separate biological replicates (n=4). *P < 0.05, **P < 0.01.

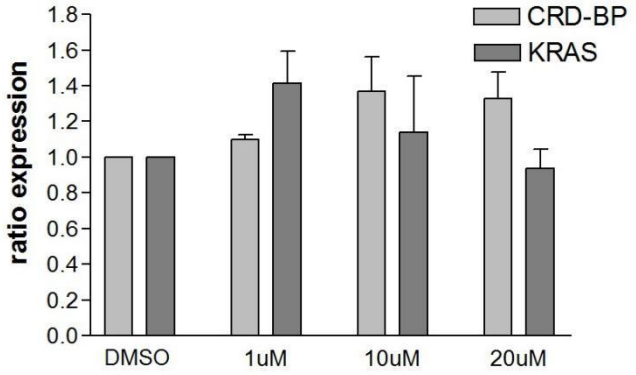

Figure 3.8 CRD-BP and KRAS protein expression in unbc143-treated SW480 cells. The levels of CRD-BP and KRAS in unbc143-treated samples, as quantified using Western blot analysis, were normalized to protein level of β–actin. SW480 colon cancer cells were treated with three different concentrations (1, 10, 20 μM) of unbc143 as described in section 3.1.1. Results were then expressed relative to DMSO-treated control as shown. Results shown were based on four separate biological replicates (n=4). Error bars indicate S.E.M.

As is shown in Figure 3.7 and Figure 3.8, both protein and mRNA levels were relatively stable when unbc143 was added to SW480 cells, indicating that unbc143 had no significant effect on KRAS protein expression in cells.

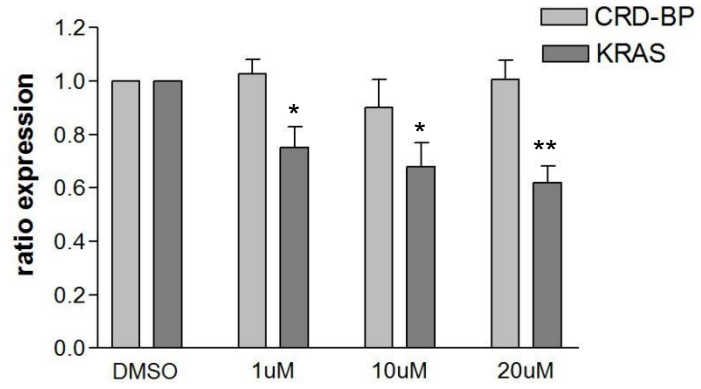

Figure 3.9 CRD-BP and KRAS mRNA expression in unbc152-treated SW480 cells. SW480 colon cancer cells were treated with three different concentrations (1, 10, 20 μM) of unbc152 as described in section 3.1.1. Results were normalized to mRNA level of β–actin and then expressed relative to DMSO-treated control as shown. Results shown were based on four separate biological replicates (n=4). Error bars indicate S.E.M.*$P < 0.05$, **$P < 0.01$.

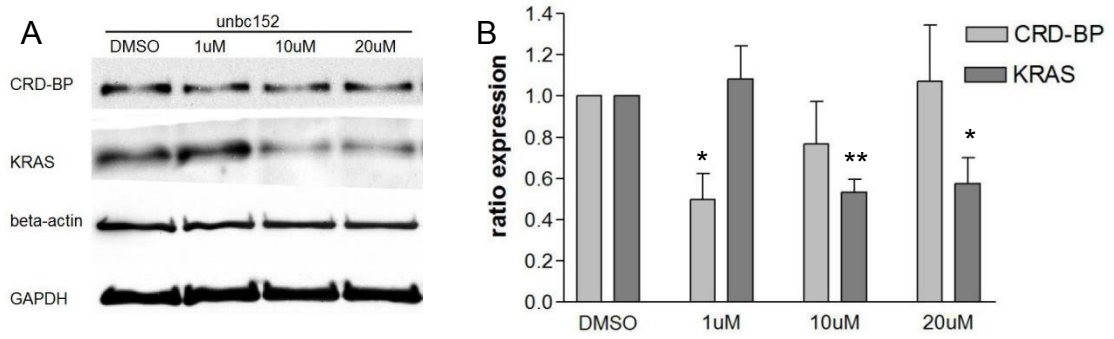

Figure 3.10 CRD-BP and KRAS protein expression in unbc152-treated SW480 cells. (A) SW480 colon cancer cells were treated with three different concentrations (1, 10, 20 μM) of unbc152 as described in section 3.1.1. Cell lysates collected were subjected to Western blot analysis as shown. The result shown is a representative of four biological replicate (n=4). (B) The levels of CRD-BP and KRAS protein levels in unbc152-treated cells were quantified and normalized to that of GAPDH and then expressed relative to the DMSO-treated control as shown. Results shown were based on (A) and three other biological replicates (n=4). Error bars indicate S.E.M. *P < 0.05, **P < 0.01.

Although changes at the KRAS mRNA levels were not as marked as the KRAS protein levels, we could still see the similar decline trend as the concentration of unbc152 increases. In fact, about 40% inhibition on KRAS mRNA expression was observed at 20 μM of unbc152 (Figure 3.9). KRAS protein levels were significantly reduced to around 50% in the presence of 10 μM unbc152 (Figure 3.10). This result is consistent with the hypothesis that unbc152 could block the interaction between CRD-BP and KRAS mRNA in cells as it did *in vitro* (Figure 2.8).

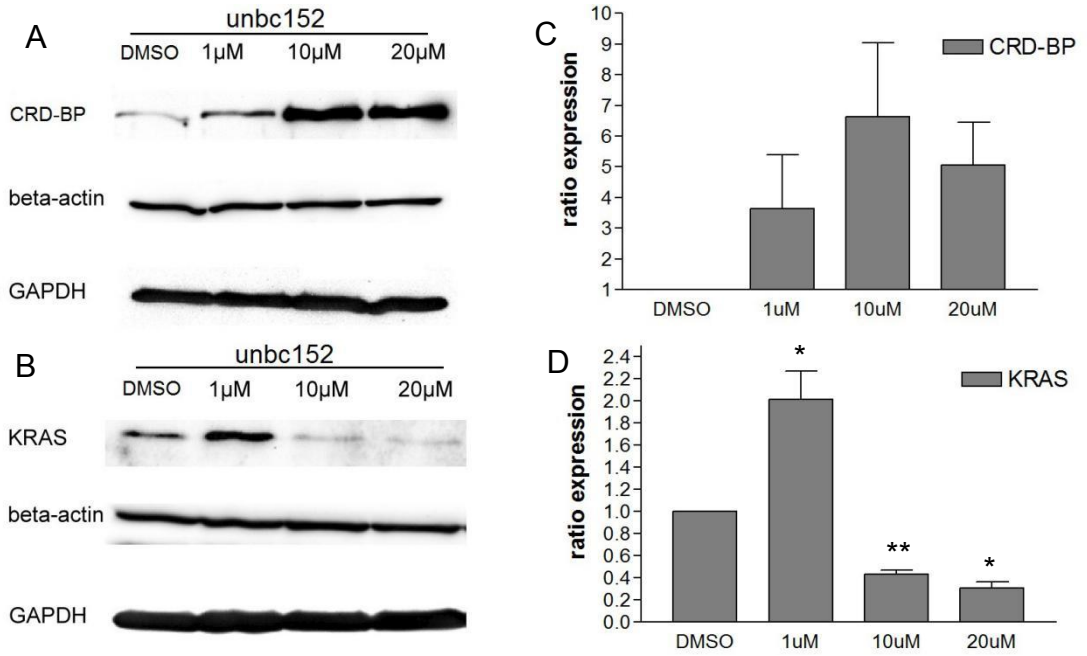

Figure 3.11 CRD-BP and KRAS protein expression in unbc152-treated HT29 cells. (A and B) HT29 colon cancer cells were treated with three different concentrations (1, 10, 20 μM) of unbc152 as described in section 3.1.1. Cell lysates collected were subjected to Western blot analysis as shown. The result shown is a representative of three biological replicates respectively (n=3). (C and D) The levels of CRD-BP and KRAS protein in unbc152-treated cells were quantified and normalized to that of β–actin and then expressed relative to the DMSO-treated control as shown. Results shown were based on four separate biological replicates, respectively (n=3). Error bars indicate S.E.M. *P < 0.05, **P < 0.01.

To assess whether the inhibitory effect of unbc152 also exists in other colon cancer cell line, I performed similar experiments on HT29 colon cancer cell line. Results showed that indeed KRAS protein levels were significantly decreased to around 40% at 10 μM of unbc152 (Figure 3.11 B and D). To my surprise, I found that a significant increase in CRD-BP protein levels (3-7 fold) in the presence of unbc152 (Figure 3.11 A and C). CRD-BP was found to up-regulate several proto-oncogene expressions through shielding their transcripts from mRNA degradation (Nielsen *et. al*., 2004; Noubissi *et. al*., 2006). CRD-BP binds to the 3'UTR and coding region of c-myc and prevents endoribonuclease attack on c-myc transcript (Doyle *et. al*., 1998). KRAS is also one of the targets that

interact with CRD-BP physically. Similarly, CRD-BP could also bind to the 3'UTR and coding region of KRAS transcript (Mongroo *et. al*., 2011; Nielsen *et. al*., 2004; Noubissi *et. al*., 2006). I propose that while unbc152 docks on CRD-BP and disable its binding affinity to KRAS mRNA, KRAS mRNA loses the normal shielding protection from CRD-BP and therefore subjected to mRNA degradation. With decreased KRAS transcript levels, less KRAS proteins are translated.

In terms of the up-regulated KRAS protein observed by unbc152 in HT29 cell lines at 1 μM, I hypothesize that there might be cell stress response happening. Stöhr *et. al*. (2006) found that CRD-BP could stabilize its specific targets (such as c-myc) by forming stress granule when cells were treated with arsenate. As an integrated stress response, c-myc transcript level in stressed cells was more than 2 folds higher than that of non-stressed cells after transcription was blocked for 1 hour. A possible explanation for my results is that at low concentration, unbc152 has no effect on most of the CRD-BP-KRAS mRNA interaction in cells; rather this dispiro pyrrolizidine molecule might induce cellular stress. KRAS mRNA might be stabilized during the cellular stress and the transcription of KRAS is up-regulated. After concentration of unbc152 is increased, the small molecule inhibitor start to play its specific role in blocking the CRD-BP-KRAS mRNA interaction and this effect overwhelmed the one of cellular stress response.

Besides KRAS expression, changes in CRD-BP expression were also observed in these experiments. CRD-BP mRNA levels in HT29 is about 19 folds lower than that in

SW480 (Mongroo *et. al.,* 2011).The relatively low expression of CRD-BP expression in HT29 cells allows changes in CRD-BP expression to be more detectable. Since the CRD-BP levels in SW480 treated with unbc152 were not consistent in each biological replicate (data not shown), I proposed that CRD-BP regulation in SW480 cells might be sensitive to different cell stages. Actually, not only the KRAS mRNA but also the other CRD-BP transcript targets could not bind to CRD-BP when CRD-BP is occupied by unbc152. The Wnt/β-catenin signaling pathway has been shown to regulate CRD-BP expression through CRD-BP promoter binding. Being involved in the Wnt/β-catenin pathway, βTrCP1 mRNA is destabilized without CRD-BP binding and inactivate β-catenin degradation (Noubissi *et. al.,* 2006). Translation of IGF2 is inhibited when CRD-BP is binding to IGF2 leader 3 mRNA. If IGF2 leader 3 mRNA is free from the CRD-BP, IGF2 would signal suppress β-catenin inhibitor function and increase β-catenin activity (Djiogue *et. al.,* 2013).

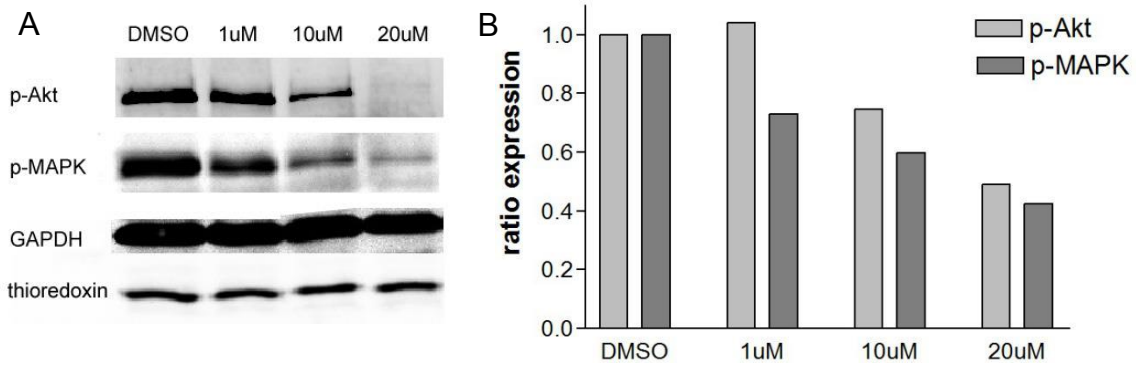

Figure 3.12 Phopho-Akt and phospho-MAPK protein expression in unbc152-treated SW480 cells. (A) SW480 colon cancer cells were treated with three different concentrations (1, 10, 20 μM) of unbc152 as described in section 3.1.1. Cell lysates collected were subjected to Western blot analysis as shown. The result shown is from one biological replicate. (B) The levels of phospho-Akt and phospho-MAPK protein in (A) were quantified and normalized to that of thioredoxin and then expressed relative to the DMSO-treated control as shown. The result shown is from one biological replicate (n=1).

As is shown in Figure 3.12, protein levels of both phospho-Akt and phospho-MAPK showed decreasing trends with the increasing dose of unbc152, and around 50% inhibition was observed in both proteins at 20 μM of unbc152.

Such results show that the suppression on KRAS expression by unbc152 leads to the inhibition of downstream KRAS signaling pathway in a KRAS-dependent manner. Since both Akt and MAPK are activated by KRAS signaling, the suppression of KRAS levels leads to inactivation of Akt and MAPK. In Raf/MEK/ERK signaling pathway, GTP-bound KRAS activates Raf protein to phosphorylate MEK (MAPK kinase), which would then phosphorylate and activate ERK (MAPK). When KRAS is mutated or over-expressed, continuously activated state of GTP-KRAS would amplify the Raf/MEK/ERK signaling pathway and disrupt normal cell differentiation and apoptosis (Dhillon *et. al.*, 2007). Courtney *et. al.* (2010) showed that KRAS is able to bind one of the PI3K subunits, p110, and activate PI3K signaling. PI3K promotes PIP2 phosphorylation to PIP3, and then phosphorylate and activate PDK1 and Akt. Activation of Akt direct- or indirectly inhibits the expression of several pro-apoptotic genes including BAD, BAX, FOXO, TSC2, GSK3 and p53, and leads to increased cell survival.

CHAPTER 4 General Discussion

4.1 Project general overview

CRD-BP (mouse), also termed IGF2BP1, IMP1 (human) and ZBP-1 (chicken), was first discovered for its high affinity for the coding region instability determinant (CRD) of c-myc mRNA and postulated to protect c-myc mRNA from endonuclease attack and RNA degradation (Bernstein *et. al.*, 1992; Lemm *et. al.*, 2002). CRD-BP is expressed during embryonic development and is barely observed after the birth. Studies show that it controls the expression of IGF2 in the late development of embryogenesis by targeting the IGF2 leader 3 mRNA and suppressing its translation (Nielsen *et. al.*, 1999). In several types of cancers including breast, testicular, lung and colorectal cancers (Doyle *et. al.*, 2000; Kato *et. al.*, 2007; Hammer *et. al.*, 2005; Ioannidis *et. al.*, 2005, Ross *et. al.*, 2001), CRD-BP was found to re-express and is involved in the regulation of cancer-related genes such as CD44, c-myc , GLI1, KRAS and MDR-1 (Vikesaa *et. al.*, 2006; Lemm *et. al.*, 2002; Noubissi *et. al.*, 2009; Mongroo *et. al.*, 2011; Mahapatra et al., 2013). Loss of CRD-BP was reported to increase cell adhesion, invadopodia formation and cell proliferation (Vikesaa *et. al.,* 2006; Ioannidis *et. al.*, 2005); however, increase of tumor cell invasion and migration was also observed in human leukemia and breast cancer with CRD-BP knockdown, indicating the essential role of CRD-BP in controlling cancer cell development (Liao *et. al.*, 2004; Gu *et. al.*, 2009).

The RAS family encodes a class of membrane-localized small GTPase and functions as signaling switch. As the RAS family member, KRAS has the highest mutational rate in

all kinds of human carcinomas. Around 30-40% of colorectal cancers harbor KRAS mutations and about 97% of KRAS mutations are located in codons 12 and 13. The most frequent mutation happens in codon 12 from GGT to GAT, which disrupts the formation of GTPase and results in constantly activated state of the GTPase (Arrington *et. al.*, 2012). Since mutation of KRAS leads to continuous binding of KRAS-GTP and failure of GTP hydrolysis, pathways related to KRAS downstream signaling such as MAPK and PI3K pathway would be constantly activated, leading to cellular effects related to oncogenesis such as cell proliferation and migration (Zenonos and Kyprianou, 2013; Dhillon *et. al.* 2007). Recent study also reported that KRAS-GTP dimers or higher order clusters are essential components to activate MAPK pathway. Elevated phosphor-Erk expression was observed by inducing artificial KRAS-GTP dimers, and the massive cell death triggered by doxycycline and MEK inhibitor could be restored by addition of dimerization of artificial KRAS-GTP dimers (Nan *et. al.*, 2015). CRD-BP binds to the coding region and 3'UTR of KRAS mRNA, and positively regulates KRAS gene expression (Mongroo *et. al.*, 2011). The major goal of this research is to identify inhibitors of CRD-BP-KRAS mRNA interaction *in vitro* and then assessing them for their potential ability to suppress KRAS expression in tumor cells.

4.2 Establishing the FP method to study CRD-BP-KRAS RNA interaction

CRD-BP consists of four hnRNP K-homology (KH) domains and two RNA recognition motifs (RRM) (Doyle *et. al.*, 1998). The KH domain is a nucleic acid

recognition and binding motif. Each KH domain harbors a highly conserved *GXXG* loop (Valverde *et. al.,* 2008). To investigate the functions of each KH domain in CRD-BP, Barnes *et. al.* (2015) introduced site-directed point mutation at the first glycine of the *GXXG* loop in each of the KH domain. According to the reported EMSA study, CRD-BP variants harboring single-point mutation retained their binding ability to c-*myc* and CD44 mRNA; however, double-point mutated variants with the exception of KH3-4 di-domain significantly reduced the binding or completely abrogated RNA binding. It was therefore hypothesized that at least two tandem KH domains are required for CRD-BP to efficiently bind to its target transcripts (Barnes *et. al.*, 2015).

To determine whether the FP method can be used to confirm the EMSA results and therefore a valid method to further study the CRD-BP-KRAS mRNA interaction, I assessed three KH variants of CRD-BP for binding to fluorescently-labeled CD44 and KRAS RNA. As shown in Figure 2.3 (D, E, and F), the previously reported binding patterns of CRD-BP to CD44 RNA using EMSA (Barnes *et. al.,* 2015) were also observed in the FP assay. For instance, using both EMSA (Barnes *et. al.*, 2015) and FP (Figure 2.3D), the KH1-2 variant exhibited no binding to CD44 RNA. Similarly, using both methods the KH3 variant (Barnes *et. al.*, 2015; Figure 2.3E) showed significantly reduced ability to bind to CD44 RNA as compared to the WT CRD-BP. Using the EMSA, the KH3-4 variant was found to have binding affinity for CD44 RNA which is comparable to the WT CRD-BP (Barnes *et. al*., 2015); however, using the FP method the KH3-4 variant was found to have slightly reduced affinity for CD44 RNA (Figure 2.3F). Such small

discrepancy could be attributed to the fact that smaller CD44 RNA (39 nt) was used in the FP method as opposed to the 194 nt CD44 RNA used in the EMSA (Barnes *et. al.*, 2015).

To gain further confidence, I also used the FP method to study CRD-BP-KRAS RNA interaction. Again, the binding patterns observed using the FP method recapitulated what were previously reported using the EMSA (Mackedenski and Lee, 2015). Using EMSA, the KH1-2 variant had no binding affinity while the KH3 variant showed significantly reduced affinity for the KRAS RNA (Mackedenski and Lee, 2015). These were also observed using the FP method (Figure 2.3A and B). Interestingly, while the KH3-4 variant showed no sign of binding affinity for the KRAS RNA (Mackedenski and Lee, 2015) using EMSA, modest binding by this variant was observed using FP (Figure 2.3C). Again, this could be due to the different sized KRAS RNAs (185 nts for EMSA and 44 nts for FP) used in the two different methods. Alternatively, the results may just reflect the differences between the two methods used in measuring molecular interactions. In EMSA, a snap-shot of molecular interaction is only observed and one does not see a dynamic molecular interaction, and any rapid dissociation would lead to an under-estimation of the binding affinity (Hellman and Fried, 2007). On the other hand, FP measurements are done in real-time and hence it can capture the dynamic molecular interaction.

In summary, I have shown that the developed FP method to study CRD-BP-RNA interaction can faithfully reproduce the EMSA results, and hence confirmed the validity in using the FP method to conveniently study CRD-BP-RNA interaction.

4.3 Identifying small molecule inhibitors for CRD-BP-KRAS RNA interaction in vitro

To identify small molecule inhibitors of CRD-BP-KRAS RNA interaction, I screened a small molecule library containing 217 dispiro pyrrolizidine/indanone derivatives that were provided by our collaborator at the University Sains Malaysia. These small molecules could be classified roughly into 7 main structures with different substituents on each structure class. However, some of the small molecules are autofluorescent and known to interfere with FP measurements (Lea and Simeonov, 2011). In my study, the autofluorescent molecules appeared to show false positive in the FP assay (Figure 2.5). The autofluorescent molecules might interrupt with the reporter fluorophore in FP assay if their excitation light and emission light spectrum regions are overlapped (Simeonov e*t. al.,* 2008). Except for the autofluorescent molecules, I found that insoluble small molecule compounds could also result in false positive signal during the FP assay (data not shown). Large particles such as insoluble compounds could result to turbidity in reaction environment and change the normal optical path of the excitation and emission light (Owicki, 2000). The insoluble compounds might also disrupt physical association between CRD-BP and KRAS mRNA in reaction resulting in false inhibitory effect in the FP assay.

SM7 displayed effective inhibitory effect with an IC_{50} of 1.18 nM in the EMSA analysis where 118 pM of KRAS and 217 nM of CRD-BP were used (Sebastian Mackedenski, unpublished data). In the FP assay at 500 nM, SM7 did not show potent

inhibitory effect (only around 30% decrease) where 10 nM of KRAS and 500 nM of CRD-BP were used. Such differences could be attributed to the differences in the properties of the two analytical methods as described in Section 4.2. Also, the sequence of SM7 is complementary to the fluorescent-labeled KRAS mRNA and therefore they might form a AON-RNA duplex in the FP assay. Although the size of AON is very small (23 nts), their binding might increase slightly the FA value, leads to less "inhibition".

4.4 Assessing inhibitory effect of AONs on CRD-BP and KRAS RNA expression in colon cancer cells

The AON SM6 and SM7 which are complementary to KRAS mRNA were designed to block CRD-BP-KRAS mRNA interaction by targeting KRAS mRNA and preventing CRD-BP association with KRAS mRNA. They have been proven to be effective in inhibiting CRD-BP-KRAS mRNA interaction *in vitro* (Sebastian unpublished data) and are expected to knockdown KRAS expression if they truly function to disrupt CRD-BP-KRAS mRNA in cells. However, these AONs were found to decrease CRD-BP protein expression largely without disrupting mRNA levels of CRD-BP and KRAS (Figure 3.4 and Figure 3.5). These results suggest that the interaction between the AONs and KRAS transcripts did not affect the stability of KRAS mRNA and protein.

King *et. al.* (2014) reported three AONs against CD44 RNA that could interrupt CRD-BP-CD44 mRNA interaction. These AONs were able to inhibit the binding of [^{32}P]-labeled CD44 RNA fragment to CRD-BP in EMSA and they were also inhibitory on CD44 mRNA expression in cells. CD44 mRNA is protected from decay upon binding of

CRD-BP (Vikesaa *et. al.,* 2006), and the AONs against CD44 RNA are expected to bind to CD44 transcripts and therefore disabled CRD-BP association with CD44 mRNA. In my hypothesis, CRD-BP and KRAS translation repressor(s) are competiting for binding to KRAS mRNA. If KRAS-specific AONs bind to KRAS transcripts, they might also compete with KRAS translation repressor(s). Only when the AONs could block CRD-BP-KRAS mRNA association without disrupting translation repressor(s) binding to KRAS mRNA, suppression of KRAS protein translation could happen. SM6 and SM7 might physically interact with KRAS transcripts at the same site which is targeted by the translation repressor(s). In this case, even if the CRD-BP dissociate from KRAS transcripts, translation repressor(s) are still unable to bind KRAS transcripts because the SM6 and SM7 may remain hybridized to KRAS mRNA.

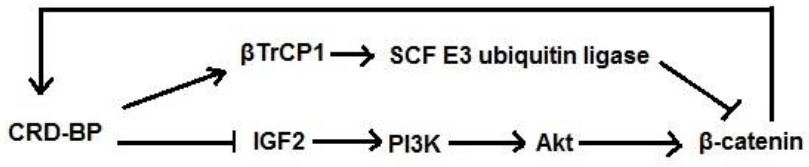

Figure 4.1 A possible feedback regulation of CRD-BP with its targets

The interaction between these AONs and KRAS mRNA might disrupt certain pathways related to the CRD-BP expression. Given that CRD-BP was knocked down to about 40% as shown in Figure 3.5. I propose the following model to explain my observations. Upon disruption of CRD-BP-KRAS mRNA interaction by the AONs, more CRD-BP is available to interact with its other targeted transcripts, and through such interaction in which CRD-BP might be feedback regulated (Figure 4.1). CRD-BP promoter is a direct target of β-catenin/TCF complex, and Wnt/β-catenin signaling could

up-regulate CRD-BP expression via CRD-BP promoter-driven transcription. With RNA silencing knockdown of β-catenin and TCF4, both CRD-BP mRNA and protein levels were decreased to around 50%, implying that both β-catenin and TCF are essential for CRD-BP expression (Noubissi *et. al.*, 2006; Gu *et. al.*, 2008). The F-box protein βTrCP1 mRNA, which is one of the four subunits of the SCF E3 ubiquitin ligase complex, is bound by CRD-BP at its 5'UTR. Binding of CRD-BP to βTrCP1 mRNA leads to accumulation of both βTrCP1 transcript and protein, promoting activation of SCF E3 ubiquitin ligase and β-catenin proteolysis (Noubissi *et. al.*, 2006). Another example is IGF2, whose translation is inactivated by CRD-BP (Djiogue *et. al.,* 2013). IGF2 interacts with insulin-like growth factor 1 receptor or insulin receptors to activate the PI3K/Akt signaling pathway. This pathway would inactivate GSK3β, which is the β-catenin inhibitor, and promote β-catenin expression. Binding of CRD-BP to IGF2 mRNA suppresses IGF2 expression, and therefore triggers GSK3β function to inhibit β-catenin. Therefore, it is possible that when more CRD-BP is available to bind βTrCP1 and IGF2 mRNAs, β-catenin would be down-regulated through the above signaling pathways resulting in the suppression of CRD-BP promoter-driven transcription.

4.5 Assessing the inhibitory effect of unbc152 on CRD-BP and KRAS expression in colon cancer cells

CRD-BP has been shown to stabilize its targeted transcripts (Vikesaa *et. al.*, 2006; Noubissi *et. al.*, 2009) or interfere with the translation of transcripts (Nielsen *et. al.*, 1999; Stöhr *et. al.,* 2012). In the CRD-BP RNA silencing experiments, KRAS mRNA levels

were found to be unaffected although CRD-BP expression was down-regulated (Figure 3.1). If KRAS mRNA is also shielded by CRD-BP, the knockdown of CRD-BP should disrupt the protection on KRAS transcripts leading to its degradation. Since CRD-BP is regulating KRAS without affecting KRAS mRNA levels, I hypothesize that CRD-BP might compete with KRAS translation suppressors in binding to KRAS transcript resulting in the up-regulation of KRAS translation. Figure 3.2 shows that loss of CRD-BP leads to the down-regulation of KRAS expression in cells, which is consistent with an earlier study by Mongroo *et. al.* (2011). The authors discovered that the p53-inducible gene CYFIP2 is negatively regulated by CRD-BP and the increased mRNA levels of CYFIP2 was observed after suppressing CRD-BP expression. KRAS inhibition induced by CRD-BP loss could be restored by knocking down CYFIP2, implying a new mechanism of KRAS regulation by CRD-BP via CYFIP2 (Mongroo *et. al.,* 2011). Besides, let-7 microRNA family targets the 3'UTR of KRAS mRNA and represses KRAS translation. Johnson *et. al.* (2005) observed that loss of let-7 microRNA results in 70% increase of RAS (N-, H- and KRAS) expression in HeLa cells. CRD-BP binds to KRAS transcript at the 3'UTR might competitively allow the translational process leading to increased KRAS expression (Johnson *et. al.*, 2005; Bell *et. al.*, 2013).

However, I was surprised to see significant down-regulation of not only the KRAS protein expression but also the KRAS mRNA levels upon treatment with unbc152. This result suggests another possible regulatory pattern in that CRD-BP could also shield KRAS transcript from RNA decay in certain circumstances. CRD-BP knockdown by

siRNA happens at the post-transcriptional level, while unbc152 functions at the post-translational level. I propose that unbc152 blocked CRD-BP-KRAS mRNA interaction by binding to CRD-BP and thereby freeing the KRAS mRNA for nucleolytic attack. The RNA silencing using siRNA might turn on or off some signaling pathways associated with CRD-BP, while these pathways might not be affected by the action of unbc152 on CRD-BP. Besides, the study by Mongroo *et. al*. (2011) had shown that CRD-BP RNA silencing leads to suppression of CRD-BP protein expression with stable pre- and mature let-7 miRNA levels. Such results, in combination with my results shown in Figure 3.1 that the suppressive effect of CRD-BP siRNA results in CRD-BP transcript degradation, suggest that there may be less amount of CRD-BP mRNA-bound let-7 miRNA. Under these circumstances, it is possible that more let-7 miRNA are free to bind to other let-7 targets such as KRAS, resulting in KRAS translation repression. In the situation where CRD-BP gene transcription is normal and CRD-BP mRNA still requires bound let-7 miRNA, and CRD-BP protein activity/function is blocked by bound unbc152, neither CRD-BP protein nor let-7 miRNA binds to KRAS transcripts. Under such circumstance, the KRAS transcripts could be exposed to nucleolytic attack resulting in decreased KRAS mRNAs and the concomitant decreased in KRAS protein expression.

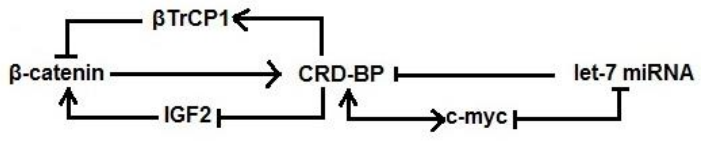

Figure 4.2 A possible mechanism for up-regulation of CRD-BP

Referring to CRD-BP silencing experiments, CRD-BP positively regulate KRAS

expression through competition with translation repressor(s). However, the KRAS expression was decreased despite an increase level of CRD-BP in the unbc152-treated experiments in HT29 colon cancer cells (Figure 3.11). For these observations, my explanation is when CRD-BP is occupied by unbc152, it might induce certain specific selectivity of CRD-BP binding, which will not happen in CRD-BP silencing. Some of the CRD-BP targets may or may not bind to CRD-BP depending on whether their binding sites on CRD-BP are still exposed (Figure 4.2). For instance, if CRD-BP is still available for c-myc mRNA binding, then c-myc expression would be elevated. Noubissi *et. al*. (2010) reported that c-myc protein is able to recognize and interact with a specific DNA sequence localized in CRD-BP promoter and promote CRD-BP transcription. In addition, c-myc is proved to negatively control mature let-7 microRNA levels, and through which targets of let-7 microRNA are up-regulated, including CRD-BP (Mongroo *et. al*., 2011). As mention in Section 4.4, CRD-BP is also regulated by Wnt/β-catenin signaling pathway. β-catenin has shown to be a necessary component in triggering CRD-BP transcription through interacting physically with the proximal CTTTG-TC element of CRD-BP promoter (Gu *et. al.*, 2008). When CRD-BP is bound by unbc152 and to some degree could not bind to its targeted mRNAs, as according to Noubissi *et. al.* (2006) and Djiogue *et. al.* (2013), βTrCP1 mRNA would be down-regulated due to the lack of protection by CRD-BP. At the same time, IGF2 expression would be increased because translation suppression trigger by CRD-BP would have disappeared. Both mechanisms will result in an elevated level of β-catenin, and therefore promote CRD-BP expression.

4.6 Unbc152, a small molecule inhibitor of CRD-BP-KRAS RNA interaction: implications for future experiments

Frequent mutation of KRAS happens in several human carcinomas, especially the colorectal cancer. Failure of normal KRAS expression disables KRAS GTPase function, and leads to the disorder of cell growth (Arrington *et. al.*, 2012; Zenonos and Kyprianou, 2013; Dhillon *et. al.* 2007). In this study, I have shown that the small molecule unbc152 is a inhibitor of CRD-BP-KRAS RNA interaction and it successfully inhibited KRAS expression in two colon cancer cell lines. To our knowledge, this is the first demonstrated small molecule capable of disrupting CRD-BP-KRAS RNA interaction *in vitro* as well as specifically suppressing KRAS expression in cancer cells. This finding is important from several perspectives. Firstly, it demonstrates the proof-of-principle that inhibiting the function of CRD-BP through disrupting its interaction with KRAS RNA can lead to decreased expression of CRD-BP-targeted gene. Secondly, unbc152 potentially represents a new class of anti-cancer drugs which act by inhibiting a new molecular pathway, a specific protein-RNA interaction.

The following are some recommended experiments using unbc152 that could be done to further understand the basic mechanism of action of unbc152 and the role of CRD-BP and KRAS in cancer biology. (1) To determine whether unbc152 can inhibit KRAS expression in different types of cancer cells. (2) To determine what other proteins (e.g. c-myc) whose expression may also be suppressed by unbc152. (3) To determine the crystal structure of unbc152 in complex with KH34 di-domain of CRD-BP.

It is important to determine whether the inhibitory effect of unbc152 on KRAS expression is truly unique to colon cancer cells. To address this, one could examine the effect of unbc152 on CRD-BP and KRAS gene expressions in a larger panel of colon cancer cell lines as well as other cancer cell lines where the protein levels of CRD-BP and KRAS are detectable. These would include pancreatic, lung and breast cancer cell lines. If the effect of unbc152 differs amongst these cell lines, then one could examine more closely the reasons behind such differences. Using unbc152 as a tool to understand such differences is important. This is because we will have a better understanding of the significance of CRD-BP-RNA interaction in the tumor development as well as whether the unbc152-type drug will be effective against the tumor in questions

As mentioned earlier, I hypothesize that in addition to KRAS mRNA the interaction between unbc152 and CRD-BP may shield some the binding sites of other CRD-BP targeted transcripts. Like KRAS, this could lead to suppressed protein expression of these targeted genes and suppressed phenotype. To address this, a global scale protein expression using proteomics could be done upon treatment of cells with unbc152. Base on the proteomics results, one could then design phenotype assays to examine the effect of unbc152 on cancer cell phenotype.

The on-going research in Dr. Lee's lab suggests that unbc152 is indeed targeting CRD-BP at the KH34 di-domain (Victor Liu, unpublished data). To confirm this, it is important to determine the crystal structure of unbc152 in complex with the KH34 di-domain. This experiment should be doable given that the KH34 di-domain of CRD-BP

in complex with β-actin RNA has been successful (Chao *et. al.*, 2010). With the crystal structure of unbc152-KH34 domain complex, one could then use the information to logically design inhibitors which can potentially be more potent than unbc152.

In addition to the above proposed experiments, animal model studies are required in the process of developing unbc152 as a potential new anti-cancer drug.

4.7 Summary

The observation that KRAS protein is suppressed by CRD-BP silencing in the absence of decreased KRAS mRNA, suggests that the regulation of CRD-BP on KRAS is at the level of post-transcription. Since CRD-BP has been shown to physically interact with KRAS RNA (Mongroo *et. al.,* 2011), there might be certain translational repressor(s) that could block KRAS translational process by competing with CRD-BP in binding to KRAS mRNA. Loss of CRD-BP allows the translational repressor(s) to interact with KRAS mRNA leading to KRAS protein repression.

In the AON transfection experiments, both SM7 and SM6 had no effect on the KRAS protein expression. Such results also support the notion that translational repressor(s) might compete with CRD-BP at the same binding sites on KRAS transcripts. Depending on whether the AONs bind to KRAS mRNAs at the translational repressor binding sites, this might lead to differential effect on the KRAS gene expression. The sequences of SM6 and SM7 complementary to KRAS mRNA might overlap with that of translation repressor(s) and inactivated the translational suppression. Surprisingly, both SM6 and SM7 knocked down CRD-BP levels dramatically to less than 50%, which

suggests the feedback regulation of CRD-BP. Accumulated CRD-BP that are free from KRAS transcripts might promote interactions with other CRD-BP binding targets, such as IGF2 and βTrCP1 mRNAs, and lead to negative regulation of CRD-BP (Noubissi *et. al.*, 2006; Djiogue *et. al.,* 2013).

The only small molecule inhibitor which was effective in cells is unbc152. Unbc152 decreases both KRAS mRNA (decreased to 60% at 20 μM) and protein levels (decreased to 40-60% at 10 μM) in colon cancer cells. This suggests that KRAS expression is regulated at the transcriptional and post-transcriptional levels. Although I earlier hypothesized that the regulation of KRAS is likely at the translational level as seen with the CRD-BP silencing experiments, it is not surprising to see that KRAS expression can also be regulated by multiple pathways under different circumstances. This is especially true where the mechanisms of actions of CRD-BP siRNAs and unbc152 are totally different. Noticeable increases of CRD-BP protein expression (3 to 7-fold increase) were observed in HT29 colon cancer cells after unbc152 treatment. Unbc152 is expected to block CRD-BP-KRAS mRNA interaction by associating with CRD-BP, which probably changes the exposed binding sites or even the tertiary structure of CRD-BP, thereby limiting CRD-BP binding ability to other targeting transcripts. In this case, not only KRAS but also other CRD-BP targeting genes might be regulated by unbc152. After associating with unbc152, some of the binding sites on CRD-BP might be shielded from certain RNAs and some might still be exposed, which might results in binding selectivity of CRD-BP. It is possible that CRD-BP binds to RNAs such as c-myc and β-catenin that

could positively feedback regulate itself, (Noubissi *et. al*., 2010; Gu *et. al*., 2008), or disable binding of RNAs such as IGF2 and βTrCP1 that negatively feedback regulate CRD-BP (Noubissi *et. al.*, 2006; Djiogue *et. al.,* 2013). In the preliminary Western blot assay of phospho-Akt and phospho-MAPK, knockdown of both proteins after unbc152 treatment indicates that unbc152 inhibitory effect on KRAS expression also down-regulates the downstream KRAS signaling pathways. Such results confirm that unbc152 can inhibit KRAS-mediated downstream signaling pathway and suggest that it could inhibit KRAS-mediated cancer cell phenotype such as cell growth.

References

Adjei AA. K-ras as a target for lung cancer therapy. J Thorac Oncol. 2008; 3 (6 Suppl 2): S160-S163.

Arrington AK, Heinrich EL, Lee W, Duldulao M, Patel S, Sanchez J, Garcia-Aguilar J, Kim J. Prognostic and Predictive Roles of KRAS Mutation in Colorectal Cancer. Int J Mol Sci. 2012; 13:12153-12168.

Bamford S, Dawson E, Forbes S, Clements J, Pettett R, Dogan A, Flanagan A, Teague J, Futreal PA, Stratton, MR, Wooster R. The COSMIC (Catalogue of Somatic Mutations in Cancer) database and website. Br J Cancer. 2004; 91: 355–358.

Barnes M, Van Rensburg G, Li WM, Mehmood K, Mackedenski S, Chan CM, King DT, Miller AL, Lee CH. Molecular insights into the Coding Region Determinant-Binding Protein-RNA interaction through site-directed mutagenesis in the heterogenous nuclear ribonucleoprotein-K-homology domains. J Biol Chem. 2015; 290: 625–639.

Bell JL, Wächter K, Mühleck B, et al. Insulin-like growth factor 2 mRNA-binding proteins (IGF2BPs): post-transcriptional drivers of cancer progression? Cell Mol Life Sci. 2013; 70: 2657-2675.

Bernstein PL, Herrick DJ, Prokipcak RD, Ross J. Control of c-myc mRNA half-life in vitro by a protein capable of binding to a coding region stability determinant. Genes Dev. 1992; 6: 642-654.

Binder R, Horowitz JA, Basilion JP, Koeller DM, Klausner RD and Harford JB. Evidence that the pathway of transferrin receptor mRNA degradation involves an endonucleolytic cleavage within the 3' UTR and does not involve poly(A) tail shortening. EMBO J. 1994; 13: 1969–1980.

Boyerinas B, Park SM, Shomron N, Hedegaard MM, Vinther J, Andersen JS, Feig C, Xu J, Burge CB, Peter ME. Identification of let-7-regulated oncofetal genes. Cancer Res. 2008; 68: 2587-2591.

Calin GA, Ferracin M, Cimmino A, Leva GD, Shimizu M, Wojcik SE, Iorio MV, Visone R, Sever NI, Fabbri M, Iuliano R, Palumbo T, Pichiorri F, Roldo C, Garzon R, Sevignani C, Rassenti L, Alder H, Volinia S, Liu C, Kipps TJ, Negrini M and Croce CM. A MicroRNA Signature Associated with Prognosis and Progression in Chronic Lymphocytic Leukemia. N Engl J Med. 2005; 353: 1793-1801.

Chae MJ, Sung HY, Kim EH, Lee M, Kwak H, Chae CH, Kim S, Park WY. Chemincal

Inhibitor Destablilize HuR Binding to the AU-Rich Element of TNF-α mRNA. Exp Mol Med. 2009; 41: 824-831.

Chao JA, Patskovsky Y, Patel V, Levy M, Almo SC, Singer RH. ZBP1 recognition of β-actin zipcode induces RNA looping. Genes Dev. 2010; 24: 148-158.

Chou CF, Mulky A, Maitra S, Lin WJ, Gherzi R, Kappes J, Chen CY. Tethering KSRP, a decay-promoting AU-rich element-binding protein, to mRNAs elicits mRNA decay. Mol Cell Biol. 2006; 26: 3695-3706.

Cogoi S, Zorzet S, Rapozzi V, Géci I, Pedersen EB, Xodo LE. MAZ-binding G4-decoy with locked nucleic acid and twisted intercalating nucleic acid modifications suppresses KRAS in pancreatic cancer cells and delays tumor growth in mice. Nucleic Acids Res. 2013; 41: 4049-4064.

Coulis CM, Lee C, Nardone V, Prokipcak RD. Inhibition of c-myc Expression in Cells by Targeting an RNA-Protein interaction using antisense oligonucleotides. Mol Pharmacol. 2000; 57: 485-494.

Courtney KD, Corcoran RB, Engelman JA. The PI3K pathway as drug target in human cancer. J Clin Oncol. 2010; 28: 1075-1083.

Crick F. Central Dogma of Molecular Biology. Nature. 1970; 22: 561-563.

Crooke RM, Graham MJ, Lemonidis KM, Whipple CP, Koo S, Perera RJ. An apolipoprotein B antisense oligonucleotide lowers LDL cholesterol in hyperlipidemic mice without causing hepatic steatosis. J Lipid Res. 2005; 46: 872-884.

Dai X, Jiang Y, Tan C. Let-7 Sensitizes KRAS Mutant Tumor Cells to Chemotherapy. PLoS One. 2015: 6; 10:e0126653. doi: 10.1371/journal.pone.0126653.

D'Agostino VG, Adami V, Provenzani A. A novel high throughput biochemical assay to evaluate the HuR protein-RNA complex formation. PLoS One. 2013; 8: e72426. doi: 10.1371/journal.pone.0072426.

Dean NM and Bennett CF. Antisense oligonucleotide-based therapeutics for cancer. Oncogene. 2003; 22: 9087–9096.

Dhillon AS, Hagan S, Rath O, Kolch W. MAP kinase signalling pathways in cancer. Oncogene. 2007; 26: 3279-3290.

Djiogue S, Nwabo Kamdje AH, Vecchio L, Kipanyula MJ, Farahna M, Aldebasi Y, Seke Etet PF. Insulin resistance and cancer: the role of insulin and IGFs. Endocr Relat Cancer. 2013; 20: R1-R17.

Doyle GA, Betz NA, Leeds PF, Fleisig AJ, Prokipcak RD, Ross J. The c-myc coding region determinant-binding protein: a member of a family of KH domain RNA-binding proteins. Nucleic Acids Res. 1998; 26: 5036–5044.

Doyle GA, Bourdeau-Heller JM, Coulthard S, Meisner LF, Ross J. Amplification in human breast cancer of a gene encoding a c-myc mRNA-binding protein. Cancer Res. 2000; 60: 2756-2759.

Fire A, Xu S, Montgomery MK, Kostas SA, Driver SE, Mello CC. Potent and specific genetic interference by double-stranded RNA in *Caenorhabditis elegans*. Nature. 1997; 391: 806-811.

Friday BB, Adjei AA. K-ras as a target for cancer therapy. Biochim Biophys Acta. 2005; 1756(2): 127-144.

Garneau NL, Wilusz J, Wilusz CJ. The highways and byways of mRNA decay. Nat Rev Mol Cell Biol. 2007; 8:113-126.

Goraczniak R and Gunderson SI. The regulatory element in the 3'-untranslated region of human papillomavirus 16 inhibits expression by binding CUG-binding protein. J Biol Chem. 2008; 283: 2286-2296.

Gray NK, Pantopoulos K, Dandekar T, Ackrell BA, Hentze MW. Translational regulation of mammalian and Drosophila citric acid cycle enzymes via iron-responsive elements. Proc Natl Acad Sci USA. 1996; 93: 4925-4930.

Gu L, Shigemasa K and Ohama K. Increased Expression of IGF II mRNA-Binding Protein 1 mRNA Is Associated with an Advanced Clinical Stage and Poor Prognosis in Patients with Ovarian Cancer. Int. J. Oncol. 2004; 24: 671–678.

Gu W, Wells AL, Pan F and Singer RH. Feedback regulation between zipcode binding protein 1 and beta-catenin mRNAs in breast cancer cells. Mol Cell Biol 2008; 28: 4963-4974.

Gu W, Pan F, Singer RH. Blocking β-catenin binding to the ZBP1 promoter represses ZBP1 expression, leading to increased proliferation and migration of metastatic breast-cancer cells. J Cell Sci. 2009; 122: 1895- 1905.

Hammer NA, Hansen Tv, Byskov AG, Rajpert-De Meyts E, Grøndahl ML, Bredkjaer HE, Wewer UM, Christiansen J, Nielsen FC. Expression of IGF-II mRNA-binding proteins (IMPs) in gonads and testicular cancer. Reproduction 2005; 130: 203-212.

Hellman LM and Fried MG. Electrophoretic Mobility Shift Assay (EMSA) for Detecting Protein-Nucleic Acid Interactions. Nat Protoc. 2007; 2: 1849– 1861.

Hu Z, Chen J, Tian T, Zhou X, Gu H, Xu L, Zeng Y, Miao R, Jin G, Ma H, Chen Y and Shen H. Genetic variants of miRNA sequences and non-small cell lung cancer survival. J Clin Invest. 2008; 118: 2600–2608.

Ioannidis P, Kottaridi C, Dimitriadis E, Courtis N, Mahaira L, Talieri M, Giannopoulos A, Iliadis K, Papaioannou D, Nasioulas G, Trangas T.Expression of the RNA-binding protein CRD-BP in brain and non-small cell lung tumors. Cancer Lett. 2004; 209: 245-250.

Ioannidis P, Mahaira LG, Perez SA, Gritzapis AD, Sotiropoulou PA, Kavalakis GJ, Antsaklis AI, Baxevanis CN,Papamichail M. CRD-BP/IMP1 expression characterizes cord blood CD34+ stem cells and affects c-myc and IGF-II expression in MCF-7 cancer cells. J Biol Chem. 2005; 280:20086-20093.

Jinek M and Doudna JA. Review Article A three-dimensional view of the molecular machinery of RNA interference. Nature. 2009; 457: 405-412.

Johnson SM, Grosshans H, Shingara J, Byrom M, Jarvis R, Cheng A, Labourier E, Reinert KL, Brown D, Slack FJ. RAS is regulated by the let-7 microRNA family. Cell. 2005; 120:635-647.

Jones RM, MacDonald ME, Branda J, Altherr MR, Louis DN, Schmidt EV. Assignment of the Human Gene Encoding Eukaryotic Initiation Factor 4E (EIF4E) to the Region q21-25 on Chromosome 4. Somat Cell Mol Genet. 1997; 23: 221-223.

Kahvejian A, Svitkin YV, Sukarieh R, M'Boutchou MN, Sonenberg N. Mammalian poly(A)-binding protein is a eukaryotic translation initiation factor, which acts via multiple mechanisms. Genes Dev. 2005; 19: 104-113.

Kato T, Hayama S, Yamabuki T, Ishikawa N, Miyamoto M, Ito T, Tsuchiya E, Kondo S, Nakamura Y, Daigo Y. Increased expression of insulin-like growth factor-II messenger RNA-binding protein 1 is associated with tumor progression in patients with lung cancer. Clin Cancer Res. 2007; 13: 434-442.

Kiledjian M, DeMaria CT, Brewer G, Novick K. Identification of AUF1 (heterogeneous nuclear ribonucleoprotein D) as a component of the alpha-globin mRNA stability

complex. Mol Cell Biol. 1997; 17: 4870-4876.

King DT, Barnes M, Thomsen D, Lee CH. Assessing Specific Oligonucleotides and Small Molecule Antibiotics for the Ability to Inhibit the CRD-BPCD44 RNA Interaction. PLoS One. 2014; 9: e91585. doi: 10.1371/journal.pone.0091585.

Lamb CA, Helguero LA, Giulianelli S, Soldati R, Vanzulli SI, Molinolo A, Lanari C. Antisense oligonucleotides targeting the progesterone receptor inhibit hormone-independent breast cancer growth in mice. Breast Cancer Res. 2005; 7: R1111-R1121.

Lea WA, Simeonov A. Fluorescence Polarization Assays in Small Molecule Screening. Expert Opin Drug Discov. 2011; 6: 17-32.

Lee, Min-Ho; Schedl, Tim. RNA-binding proteins. WormBook. 2006:1-13.

Leech SH, Olie RA, Gautschi O, Simões-Wüst AP, Tschopp S, Häner R, Hall J, Stahel RA, Zangemeister-Wittke U. Induction of apoptosis in lung cancer cells following bcl-xL antisense treatment. Int J Cancer. 2000; 86:570-576.

Leeds P, Kren BT, Boylan JM, Betz NA, Steer CJ, Gruppuso PA, Ross J. Developmental regulation of CRD-BP, an RNA-binding protein that stabilizes c-myc mRNA in vitro. Oncogene. 1997; 14: 1279-1286.

Lemm I, Ross J. Regulation of c-myc mRNA decay by translational pausing in a coding region instability determinant. Mol Cell Biol. 2002; 22: 3959-3969.

Lewis MA, Quint E, Glazier AM, Fuchs H, De Angelis MH, Langford C, van Dongen S, Abreu-Goodger C, Piipari M, Redshaw N, Dalmay T, Moreno-Pelayo MA, Enright AJ, Steel KP. An ENU-induced mutation of miR-96 associated with progressive hearing loss in mice. Nat Genet. 2009; 41: 614-618.

Liao B, Patel M, Hu Y, Charles S, Herrick DJ, Brewer G. Targeted Knockdown of the RNA-binding Protein CRD-BP Promotes Cell Proliferation via an Insulin-like Growth Factor II-dependent Pathway in Human K562 Leukemia Cells. J Biol Chem. 2004, 279: 48716-48724.

Luedtke NW and Tor Y. Fluorescence-based methods for evaluating the RNA affinity and specificity of HIV-1 Rev-RRE inhibitors. Biopolymers. 2003; 70: 103-119.

Maas S and Rich A. Changing genetic information through RNA editing. Bioessays. 2000; 22: 790-802.

Mackedenski SJ and Lee CH. Investigating the molecular interaction between KRAS mRNA and RNA binding protein CRD-BP. Mol Cell Biol. 2015; 75: doi: 10.1158/1538-7445.

Mahapatra L, Mao C, Andruska N, Zhang C, Shapiro DJ. High-Throughput Fluorescence Anisotropy Screen for Inhibitors of the Oncogenic mRNA Binding Protein, IMP-1. J Biomol Screen. 2013; doi: 10.1177/ 1087057113499633.

Mehmood K, Akhtar D, Mackedenski S, Wang C, Lee CH. Inhibition of GLI1 Expression by Targeting the CRD-BP-GLI1 mRNA Interaction Using a Specific Oligonucleotide. Mol Pharmacol. 2016; 89: 606-617.

Mongroo PS, Noubissi FK, Cuatrecasas M, Kalabis J, King CE, Johnstone CN, Bowser MJ, Castells A, Spiegelman VS, Rustgi AK. IMP-1 displays crosstalk with K-Ras and modulates colon cancer cell survival through the novel pro-apoptotic protein CYFIP2. Cancer Res. 2011; 71: 2172–2182.

Nan X, Tamgüney TM, Collisson EA, Lin LJ, Pitt C, Galeas J, Lewis S, Gray JW, McCormick F, Chu S. Ras-GTP dimers activate the Mitogen-Activated Protein Kinase (MAPK) pathway. Proc Natl Acad Sci U S A. 2015; 112: 7996-8001.

Nielsen J, Christiansen J, Lykke-Andersen J, Johnsen AH, Wewer UM, Nielsen FC. A family of insulin-like growth factor II mRNA-binding proteins represses translation in late development. Mol Cell Biol. 1999; 19: 1262–1270.

Nielsen J, Kristensen MA, Willemoes M, Nielsen FC, and Christiansen J. Sequential dimerization of human zipcode-binding protein IMP1 on RNA: a cooperative mechanism providing RNP stability. Nucleic Acids Res. 2004; 32, 4368–4376.

Noubissi FK, Elcheva I, Bhatia N, Shakoori A, Ougolkov A, Liu J, Minamoto T, Ross J, Fuchs SY, Spiegelman VS. CRD-BP mediates stabilization of betaTrCP1 and c-myc mRNA in response to beta-catenin signalling. Nature. 2006; 441: 898-901.

Noubissi FK, Goswami S., Sanek NA, Kawakami K, Minamoto T, Moser A, Grinblat Y, and Spiegelman, VS. Wnt signaling stimulates transcriptional outcome of the hedgehog pathway by stabilizing GLI1 mRNA. Cancer Res. 2009; 69: 8572–8578.

Owicki JC. Fluorescence polarization and anisotropy in high throughput screening: perspectives and primer. J Biomol Screen. 2000; 5: 297-306.

Palanisamy V, Park NJ, Wang J, Wong DT. AUF1 and HuR Proteins Stabilize

Interleukin-8 mRNA in Human Saliva. J Dent Res. 2008; 87: 772–776.

Parker R and Song H. The enzymes and control of eukaryotic mRNA turnover. Nat Struct Mol Biol. 2004; 11: 121-127.

Rodenhuis S, Slebos RJ, Boot AJ, Evers SG, Mooi WJ, Wagenaar SS, van Bodegom PC, Bos JL. Incidence and possible clinical significance of K-ras oncogene activation in adenocarcinoma of the human lung. Cancer Res. 1988; 48: 5738–5741.

Ross J, Lemm I and Berberet B. Overexpression of an mRNA-binding protein in human colorectal cancer. Oncogene. 2001; 20: 6544-6550.

Shen J, Ambrosone CB and Zhao H. Novel genetic variants in microRNA genes and familial breast cancer. Int J Cancer. 2009; 124: 1178–1182.

Stöhr N, Lederer M, Reinke C, Meyer S, Hatzfeld M, Singer RH, Hüttelmaier S. ZBP1 regulates mRNA stability during cellular stress.The J Cell Biol. 2006; 175: 527–534.

Stöhr N, Köhn M, Lederer M, Glass M, Reinke C, Singer RH, Hüttelmaier S. IGF2BP1 promotes cell migration by regulating MK5 and PTEN signaling. Genes Dev. 2012; 26: 176-189.

Simeonov A, Jadhav A, Thomas C, Wang Y, Huang R, Southall N, Shinn P, Smith J, Austin C, Auld D, Inglese J. Fluorescence spectroscopic profiling of compound libraries. J Med Chem. 2008; 51: 2363–2371.

Simões-Wüst AP, Schürpf T, Hall J, Stahel RA, Zangemeister-Wittke U. Bcl-2/bcl-xL bispecific antisense treatment sensitizes breast carcinoma cells to doxorubicin, paclitaxel and cyclophosphamide. Breast Cancer Res Treat. 2002; 76: 157-166.

Sparanese D and Lee CH. CRD-BP shields c-myc and MDR-1 RNA from endonucleolytic attack by a mammalian endoribonuclease. Nucleic Acids Res. 2007; 35: 1209-1221.

Taft RJ, Pang KC, Mercer TR, Dinger M and Mattick JS. Non-coding RNAs: regulators of disease. J Pathol. 2010; 220: 126–139.

Tazi J, BakkourN, Stamm S. Alternative Splicing and Diseases. Biochim Biophys Acta. 2009; 1972: 14-26.

Valencia-Sanchez MA, Liu J, Hannon GJ, Parker R.Control of translation and mRNA degradation by miRNAs and siRNAs. Genes Dev. 2006; 20: 515-524.

Valverde R, Edwards L, Regan L. Structure and function of KH domains. FEBS J. 2008; 275: 2712–2726.

Veres G, Junker U, Baker J, Barske C, Kalfoglou C, Ilves H, Escaich S, Kaneshima H, Böhnlein E. Comparative analyses of intracellularly expressed antisense RNAs as inhibitors of human immunodeficiency virus type 1 replication. J Virol. 1998; 72: 1894–1901.

Vikesaa J, Hansen TV, Jønson L, Borup R, Wewer UM, Christiansen J, Nielsen FC. RNA-binding IMPs promote cell adhesion and invadopodia formation. Embo J. 2006; 25: 1456-1468.

Yisraeli JK. VICKZ proteins: a multi-talented family of regulatory RNA-binding Proteins. Biol Cell. 2005; 97: 87–96.

Zenonos K and Kyprianou K. RAS signaling pathways, mutations and their role in colorectal cancer. World J Gastrointest Oncol. 2013;5: 97-101.